3D Fluorescence Spectroscopy and Its Applications

Nathalie Locquet and Christophe B.Y. Cordella
UMR PNCA INRA AgroParisTech, Université Paris-Saclay, Paris, France

Abderrahmane Aït-Kaddour
INRA, VetAgro Sup, UMRF, Université Clermont Auvergne, Aurillac, France

This article focuses on 3D fluorescence spectroscopy. After defining its principle, we then look at the factors which influence the phenomenon of fluorescence. There follows a brief discussion of the principal chemometric techniques implemented to manipulate and exploit fluorescence data, which have different and specific properties. A new article will describe the main endogenous fluorophores found in certain food, biological and environmental matrices, as well as exogenous fluorophores. Frontal fluorescence has seen considerable development during the past 15 years in a wide variety of fields, which is why we shall also be focusing on its principal applications in terms of the objectives of different studies: classification, authentication, quality control or process monitoring indicators. Fluorescence data generate a spectral fingerprint that can characterise samples within a very large space of variability, such as that which is inherent in food samples. Fluorescence spectroscopy can thus be used in a broad range of applications involving biological samples, animal tissues or environmental samples. Most of these applications are still qualitative, although quantitative methods are available. It is generally acknowledged that 3D fluorescence fingerprinting is more suitable for recognition, classification or detection processes when there is a need to save time and achieve optimum sensitivity. With the recent development of big data and BI, frontal fluorescence spectroscopy will soon benefit from the considerable power of artificial intelligence technologies.

1 INTRODUCTION

The phenomenon of luminescence has been known since ancient times, and it has since been found that when diamonds are exposed to the sun they glow for several minutes in the dark. Another example is the 'glossy worms' that figured in different mythologies.[1,2] These are probably the first known manifestations of phosphorescence. It was not until 1664 that Vincenzo Cascariolo, a shoemaker from Bologna (Italy), rediscovered the phenomenon in calcined stones containing calcium sulfide and barium.[3] Luminescence also includes a second radiative phenomenon, fluorescence, a phenomenon whose name was invented in 1852 by the English physicist George Gabriel Stokes after observing that fluorite crystals of calcium fluoride emit blue light when illuminated under ultraviolet light.[3] Since then, fluorescence has also been observed in living beings, when it is referred to as bioluminescence. This is particularly the case of the jellyfish *Aequorea victoria*, which lives on the west coast of the USA and synthesizes a protein (green fluorescent protein – GFP) that has fluorescent properties and gives its host purple hues. Osamu Shimomura was the first to highlight the existence of this protein that has since revolutionized molecular biology because of its numerous applications.[2] From a physical point of view, fluorescence is the emission of light at a given wavelength by an object or living being; it is the consequence of energy being absorbed at an excitation wavelength that

Encyclopedia of Analytical Chemistry, Online © 2006–2018 John Wiley & Sons, Ltd.

This article was published in the *Encyclopedia of Analytical Chemistry* in 2018 by John Wiley & Sons, Ltd.
DOI: 10.1002/9780470027318.a9540

is specific to some of the molecules in the object. In the case of living beings, this phosphorescence may be due to biochemical reactions or fluorescence but is most often due to the emission of light by a protein in the body, i.e. GFP protein in *Aequorea victoria* or dsRed protein synthesized by a coral of the *Discosoma genus*. One of the most widespread applications seen today is fluorescence spectroscopy, particularly because of its versatility and speed. Using this technique, it is possible to record the emission of light produced during luminescence over a range of wavelengths that are generally in the visible range. These recordings are called fluorescence spectra. When these recordings are made for several excitation wavelengths, the juxtaposed collection of fluorescence spectra forms a three-dimensional representation of the fluorescence intensities detected (x: emission; y: excitation; z: fluorescence intensity). These are referred to as 3D spectra or an excitation emission matrix (EEM).[4–7]

Historically, 3D fluorescence analysis has emerged after lengthy technological developments during which improvements to technology, optics, and computer quality have made it possible to collect emission spectra over broad ranges of excitation and emission wavelengths. The first recordings were limited to a single excitation wavelength at any one time and one or more emission wavelengths. Today, all commercial instruments can enable multiple acquisitions of both excitation and emission wavelengths.

This article focuses on 3D fluorescence spectroscopy, also known as emission–excitation fluorescence spectroscopy. Thus, after defining its principle, we shall be focusing on the usefulness of this type of fluorescence excitation mode in terms of its applications. Because this type of analysis generates large quantities of data, it is necessary to use rapid and multidimensional data processing methods in order to better understand the value of this method when analyzing and characterizing complex samples.

2 DEFINITIONS AND SPECIFICATIONS

2.1 What Is Fluorescence? A Definition

Fluorescence is an athermic phenomenon, which results from the emission of light by objects that are living or not, after the absorption of light. The light thus generated is 'cold' when compared with the so-called 'hot' light or incandescence that is produced by a rise in body temperature. Molecules reach an excited state by absorbing a photon. A return to the ground state can be achieved in different ways; one is the emission of photons at a wavelength higher than the excitation wavelength, thus producing the fluorescence phenomenon. Fluorescence is one of the several possible routes for molecular relaxation. The principle of fluorescence is explained by Jablonski's diagram (Figure 1). At room temperature, most molecules occupy the lowest vibrational level of the fundamental electronic state or S_0.[8] In any molecular electromagnetic spectroscopy, including fluorescence spectroscopy, molecules populating the fundamental energy level S_0 are excited by the absorption of a photon

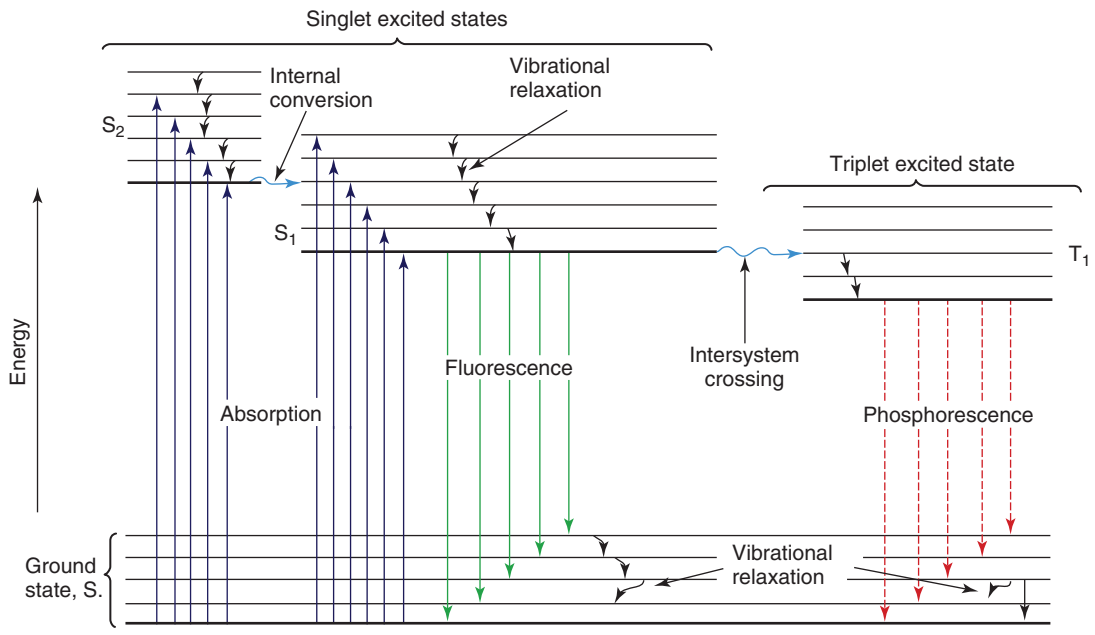

Figure 1 Jablonski diagram.

Encyclopedia of Analytical Chemistry, Online © 2006–2018 John Wiley & Sons, Ltd.

This article was published in the *Encyclopedia of Analytical Chemistry* in 2018 by John Wiley & Sons, Ltd.
DOI: 10.1002/9780470027318.a9540

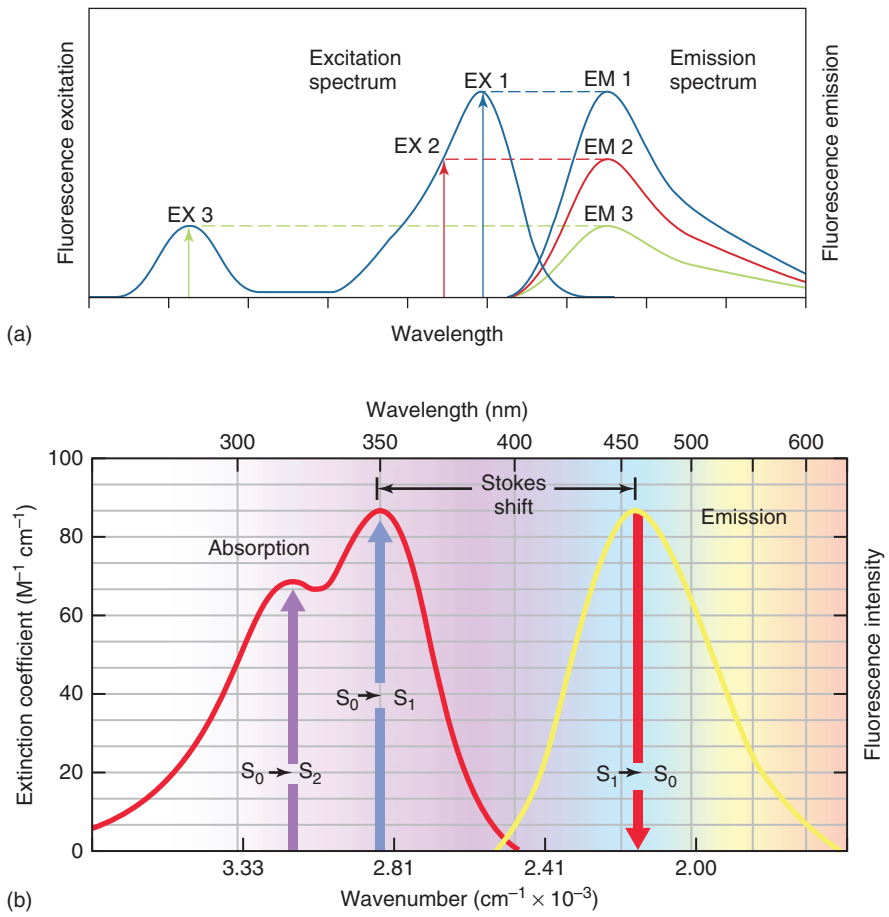

Figure 2 (a) Excitation of a fluorophore at three different wavelengths (EX 1, EX 2, EX 3) does not change the emission profile but does produce variations in fluorescence emission intensity (EM 1, EM 2, EM 3) that correspond to the amplitude of the excitation spectrum. (b) An example: a quinine absorption and emission fluorescence spectra.

will gradually populate one or more higher energy levels. These new excited electronic states are singlet states denoted S_x; $x = 1$, 2, etc. Each molecule is excited for a characteristic period of time. The next step may be either vibrational relaxation or internal conversion that permits the electron to return to the lowest vibrational state of the excited state, from S_2 to S_1 (Figure 1), which is referred to as nonradiative transition. There is a loss of vibrational energy whose origin corresponds to collisions between the excited molecule and other surrounding molecules. To put it another, during the phenomenon of phosphorescence, triplet-singlet transition requires a reorientation of spin, hence a longer transition that can range from a millisecond to a second. Fluorescence does not require a reorientation of spin and the phenomenon occurs within a few picoseconds or even a few nanoseconds. Any reorientation consumes energy that is transferred to the molecular environment. Transitions from S to T, or from T to S, are referred to as *intersystem crossing*, and from S to S or from T to T, *internal conversion*.

Finally, the emission of fluorescence occurs 10^{-8} s after excitation when the electron returns to the most stable fundamental level, S_0. The emitted light has a wavelength that corresponds to the energy difference between the two electronic levels concerned. The emission wavelength is greater than the excitation wavelength, due to the energy loss known as *Stokes' Shift* (Figure 2). Fluorescent molecules are called fluorophores; they mostly contain aromatic rings with π-linked delocalized electrons. In liquid media, in particular, the emission wavelength is greater than the excitation wavelength because the molecule returns to the ground state from the lowest vibration level of the excited state, a phenomenon referred to as Kasha's rule.

2.2 The Different Types of Fluorescence Spectra

Different types of fluorescence spectra may be encountered: excitation spectra, emission spectra, and 3D

Encyclopedia of Analytical Chemistry, Online © 2006–2018 John Wiley & Sons, Ltd.

This article was published in the *Encyclopedia of Analytical Chemistry* in 2018 by John Wiley & Sons, Ltd.
DOI: 10.1002/9780470027318.a9540

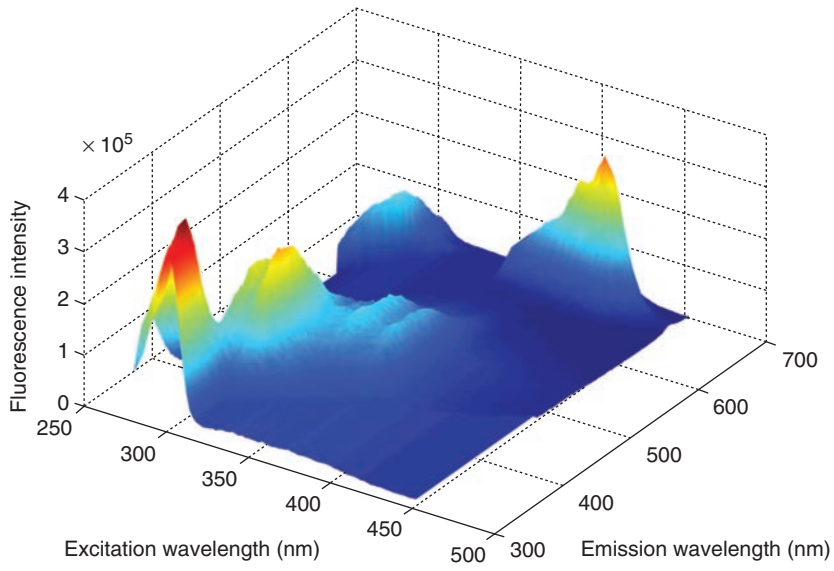

Figure 3 3D front-face fluorescence spectra moroccan olive oil (3D view).

spectra including emission–excitation matrices (EEM) and synchronous fluorescence spectra.[1,9]

An *excitation spectrum* is indicative of a variation in the intensity of the emission measured at a fixed wavelength while the excitation wavelength advances over a longer or smaller wavelength range. Optimum installation of the instrument should deliver excitation light as close as possible to the absorption spectrum of the fluorophore. Corrections to the apparatus are, therefore, necessary in many cases because the excitation spectrum is disturbed by variations in the incident intensity with the wavelength. The corrected excitation spectrum is, therefore, identical to the absorption spectrum, provided that the solution under analysis only contains one molecular species in the ground state. If there are several molecular species or several chemical oxidation states, or protonated-deprotonated states of a single species, the two corrected absorption and excitation spectra are no longer superimposable; it may be interesting to compare them (Figure 2).

An *emission spectrum* reflects the probability distribution of the various transitions from the lowest vibrational level of S_1 toward the various vibrational levels of S_0. It, therefore, corresponds to a variation of the luminescence light emission intensity as a function of the fixed excitation wavelength (Figure 2). A fluorescence emission spectrum is characteristic of a given compound.

An *absorption spectrum* results from the partial absorption of certain wavelengths of the incident excitation beam. The missing frequencies are those that best characterize the energy levels of the sample. Once corrections to the instrumentation appropriate to the analysis have been performed, the absorption spectrum can replace the fluorescence excitation spectrum.

A *3D fluorescence spectrum* is an EEM. When the excitation and emission monochromators are used successively, it is possible to measure emission spectra for different excitation wavelengths. This results in a collection of emission spectra at different excitation wavelengths with a constant step. Therefore, the EEM obtained has two dimensions: excitation wavelengths and emission wavelengths. Fluorescence matrices provide a type of fluorescence map of all the fluorophores in a mixture, thus enabling their concomitant characterization (Figures 3 and 4).

Synchronous fluorescence spectra have the advantage of being able to characterize several fluorophores from a single spectrum and thus constitutes a good compromise between EEM spectra and the standard acquisition of excitation and emission fluorescence spectra. Unlike EEM spectra, a fixed wavelength difference of $\Delta\lambda$ between the excitation wavelength λ_{ex} and the emission wavelength λ_{em} is used for spectral acquisition while respecting the following constraint: $\lambda_{em} = \Delta\lambda + \lambda_{ex.}$[10,11] The spectrum is measured at the excitation wavelengths defined by λ_{ex1}, λ_{ex2}, …, λ_{exj}, and the emission wavelengths will be: $\lambda_{em1} = \lambda_{ex1} + \Delta\lambda$; $\lambda_{em2} = \lambda_{ex2} + \Delta\lambda$, etc.

Synchronous spectra can, therefore, be observed as an oblique band of the excitation–emission surface (Figure 5). $\Delta\lambda$ is also called *offset* and can be changed.[12] According to the scanning mode applied between the excitation and emission monochromators, three types of synchronous fluorescence spectra[13] may be found. Scanning of the excitation and emission monochromator

Encyclopedia of Analytical Chemistry, Online © 2006–2018 John Wiley & Sons, Ltd.

This article was published in the *Encyclopedia of Analytical Chemistry* in 2018 by John Wiley & Sons, Ltd.
DOI: 10.1002/9780470027318.a9540

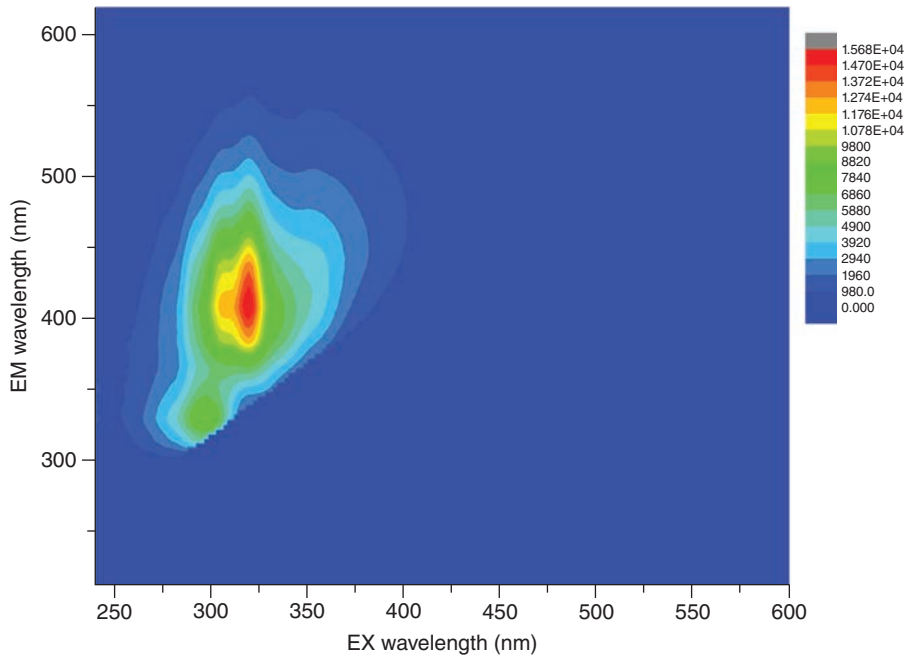

Figure 4 3D fluorescence spectra canola oil (contour map) (own spectra).

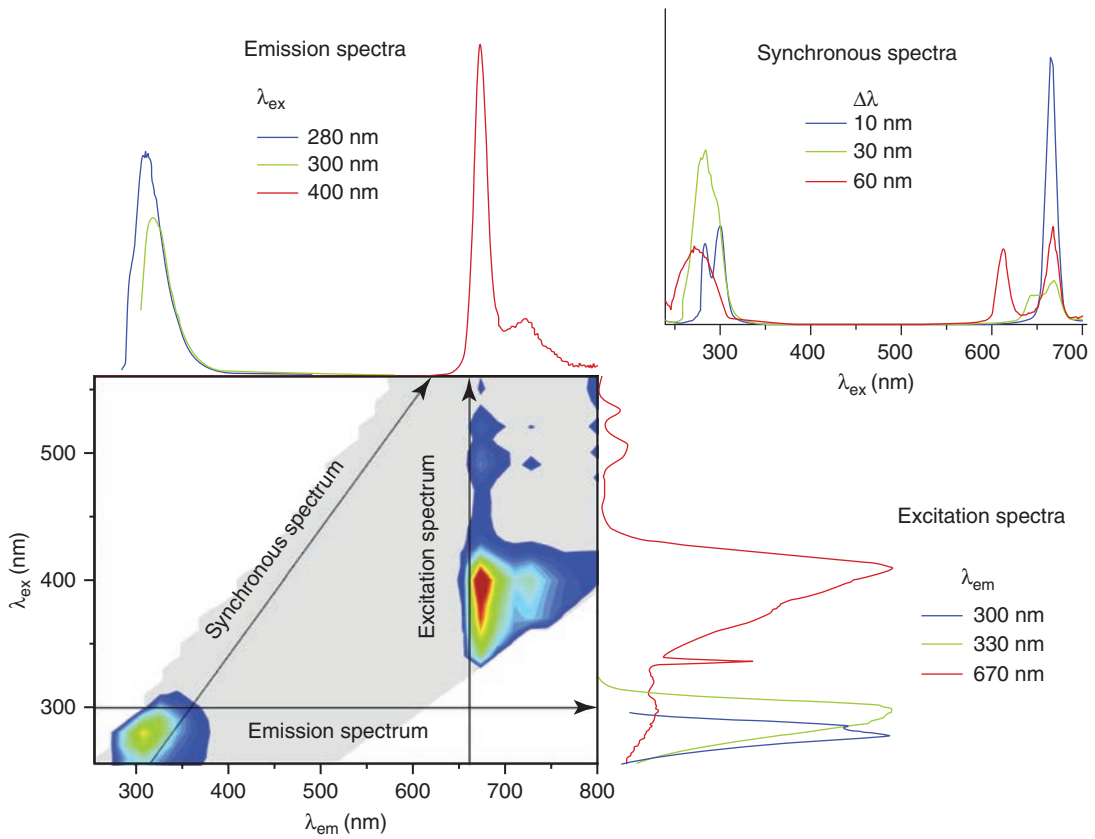

Figure 5 Different types of fluorescence spectra between 3D fluorescence spectra and synchronous spectra. (Source: Sikorska, https://www.intechopen.com/books/olive-oil-constituents-quality-health-properties-and-bioconversions/analysis-of-olive-oils-by-fluorescence-spectroscopy-methods-and-applications. Licensed under CC BY 3.0.[12])

Encyclopedia of Analytical Chemistry, Online © 2006–2018 John Wiley & Sons, Ltd.

This article was published in the *Encyclopedia of Analytical Chemistry* in 2018 by John Wiley & Sons, Ltd.
DOI: 10.1002/9780470027318.a9540

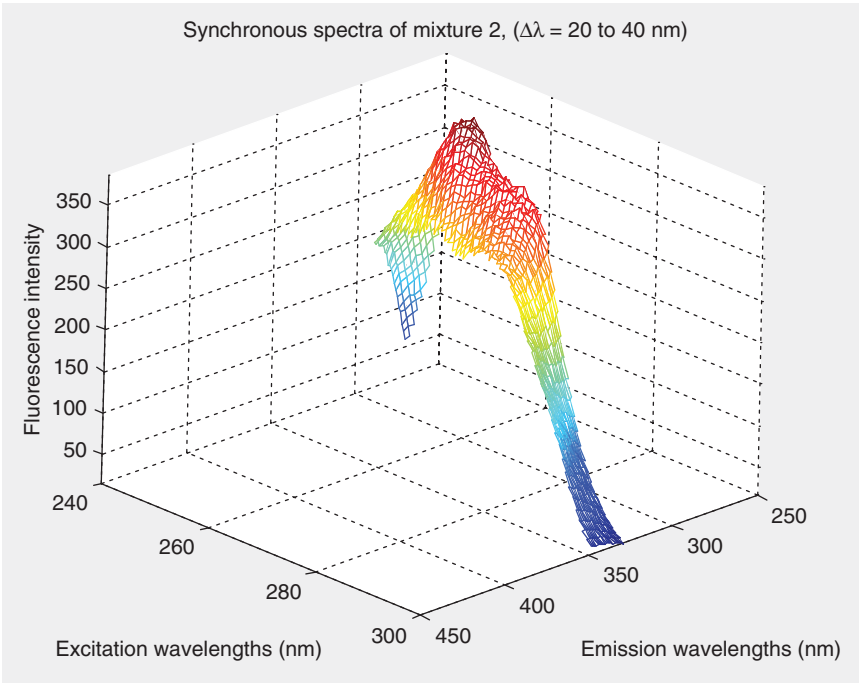

Figure 6 Synchronous spectrum, building in progress.

can be achieved using a constant wavelength shift $\Delta\lambda$, with a shift in frequency or constant energy $\Delta\nu$ or at different speeds. When the 'offset' varies with the same pitch a partial 3D spectrum is obtained, as shown in Figure 6.[13,14] This mode of acquisition is the most widespread in the literature.

Synchronous fluorescence spectroscopy (SFS) has many advantages: It provides more complete information on fluorophore mixtures, and it enables the production of finer spectral bands, a simplification of emission spectra, a reduction in the spectral change for a given analyte and compensation for Rayleigh and Raman scattering. Rapid and practical to use, synchronous fluorescence spectra (Figure 6) are a good compromise versus total luminescence spectra, i.e. EEMs. SFS is often used to characterize mixtures and has numerous applications in the field of oil chemistry. It has recently been introduced for food analysis and has encountered considerable success.[15–17] Although many studies have been conducted using SFS, only a few of them have simultaneously considered different offsets. In this article, therefore, we have only looked at studies presenting a global analysis of 3D synchronous spectra.

The 3D spectrum is generally reshaped from a series of emission, excitation, or synchronous spectra in order to generate a response surface that groups all fluorescence intensities within a selected region. However, there are several drawbacks to this type of acquisition:

1. Acquisition is slow because of wavelength scanning, and a higher speed implies a reduction in signal quality as the signal-to-noise ratio changes inversely with the ratio of scanning speed to acquisition time, etc.
2. The smaller the wavelength step, the longer the time required for analysis.

The different fluorescence spectra described above can be obtained using a variety of systems, such as the Hitachi F4500, Perkin-Elmer LS50B, Fluoromax 4 from Horiba Scientific, Xenius from Safas, or the FS5 from Edinburgh Instruments. Some instruments enable the rapid acquisition of 3D spectra in less than a minute because they are equipped with a charge coupled device (CCD) detector. Here also, the speed of acquisition is inversely proportional to sensitivity (Aqualog – Horiba Scientific). The range of excitation wavelengths, associated steps, and bandwidths and the range of emission wavelengths need to be defined. Using this type of instrument, a large number of emission spectra with a regular pitch of excitation wavelengths can be recorded.

2.3 Spectral Acquisition Mode

The sample is presented for measurement depending on the optical organization of the instrument which requires orientation with respect to the exciting light.

Encyclopedia of Analytical Chemistry, Online © 2006–2018 John Wiley & Sons, Ltd.

This article was published in the *Encyclopedia of Analytical Chemistry* in 2018 by John Wiley & Sons, Ltd.
DOI: 10.1002/9780470027318.a9540

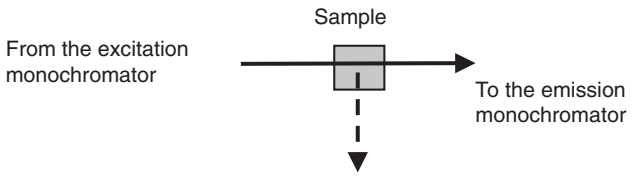

Figure 7 Schema of right-angle fluorescence.

2.3.1 Right-angle Fluorescence

When light passes through the sample, fluorescence can be disturbed or decreased by absorbance phenomena (Figure 7). The sample must, therefore, be diluted so that absorbance goes below 0.05. Right-angle fluorescence is, therefore, not suitable for opaque solids, powders, or highly viscous samples.

2.3.2 Front-face Fluorescence

To avoid dilution and absorption problems, the solution is to present the sample under incident light at an angle of less than 90° (Figure 8), so that measurements are performed in a way that is similar to ATR-infrared spectroscopy (ATR – attenuated total reflection). This is a specific recording mode in infrared spectroscopy that uses a crystal as a support for evanescent wave transmission which is produced by exciting light on the crystal sample holder from the incidence angle point of view. It can thus overcome the drawbacks right-angle fluorescence spectroscopy by modifying the angle of incidence of the exciting light by orienting the sample holder in a particular way. This angle is usually 56°, in which case it is frontal fluorescence.[18] Excitation and emission occur on the same optical surface of the cuvette. The light penetrates by a few microns. The sample may be opaque, but it must be homogeneous so that the surface characteristics will be representative of the entire sample.[8,19]

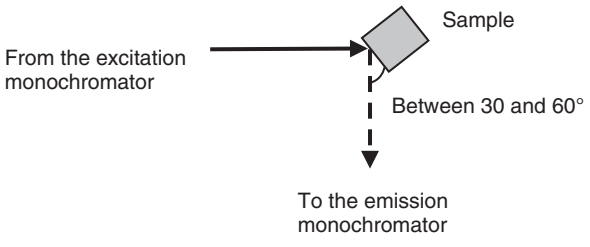

Figure 8 Schema of front-face fluorescence.

3 FACTORS AFFECTING FLUORESCENCE

3.1 Fluorescence Inhibition

Inhibition is any process that causes a decrease in fluorescence. It is defined as a loss of fluorescence signal due to short-range interactions between the fluorophore and the local molecular environment, including other fluorophores. There are four types of inhibition: filter effect, excimer effect, and static and dynamic inhibition (Figure 9a). A filter effect is caused by absorption of the fluorescence emitted due to reabsorption within the solution. The excimer effect is a phenomenon that occurs during excimer formation (Figure 9b) because of the collision of two identical molecules, the former in an excited state and the latter in ground state.[1] Static inhibition is the formation of a complex between the fluorescent molecule and an inhibitory species that leads to the decrease in fluorescence intensity. Dynamic inhibition is collisional inhibition during the lifetime of the excited state between the fluorescent molecule and inhibitory molecules, resulting in a decrease in fluorescence in terms of both intensity and half-life.

3.2 Environmental Conditions

Fluorescence spectroscopy is influenced by environmental conditions such as polarity, pH, and temperature (Figure 10).[1] The solvent has an influence on the reaction rate, the position of a chemical equilibrium, and the spectral bands recorded. Polarity characterizes the state of a molecule with positive and negative charges. The more the charges are distributed to one side or the other of a molecule or bond, the more it will be polar and vice versa; if the charges are distributed in a completely symmetrical way, the molecule will be nonpolar. In a polar environment, the fluorophore has a larger electric dipole moment in the excited state than in the ground state.[8] After excitation, dipoles from the solvent can be reoriented around the excited state. As the polarity of the solvent increases, this effect becomes more pronounced, resulting in emissions at lower energies or higher wavelengths. Generally, in a polar environment, the emission spectrum will see its maximum shift toward the highest wavelengths. Nonpolar molecules such as unsubstituted aromatic hydrocarbons are less sensitive to solvent polarity.[8] As polarity increases, the wavelength at maximum fluorescence increases and causes expansion of the Stokes phenomenon. One of the effects of polarity is hydrogen bonding.[1] The fluorescence of aromatic compounds with acidic or basic substituent rings is often pH-dependent. Wavelength and emission intensity are different depending on whether the molecule is protonated or deprotonated. Both quantum yield and excitation and emission spectra may be modified

Encyclopedia of Analytical Chemistry, Online © 2006–2018 John Wiley & Sons, Ltd.

This article was published in the *Encyclopedia of Analytical Chemistry* in 2018 by John Wiley & Sons, Ltd.
DOI: 10.1002/9780470027318.a9540

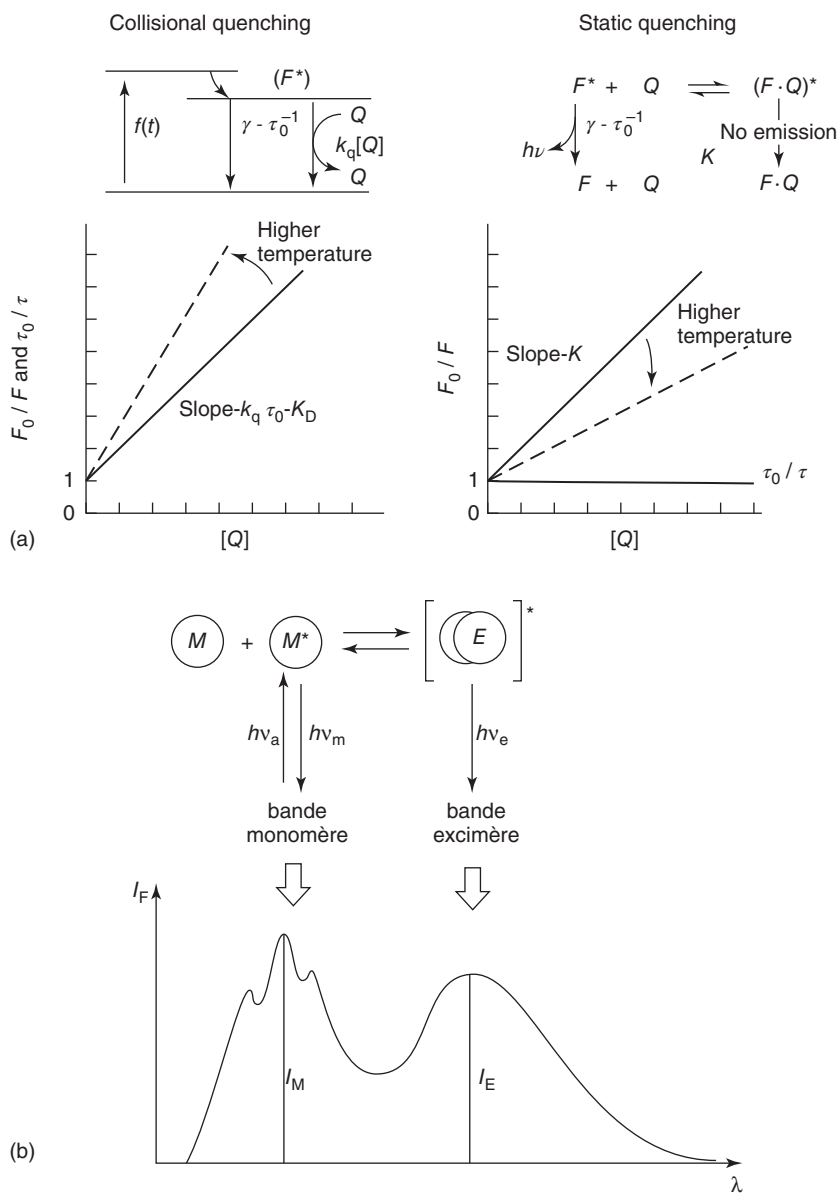

Figure 9 (a) Quenching schema. (b) Diagram of excimer formation according to Ref. 1. (Reproduced with permission from Valeur, B.: Invitation à la fluorescence moléculaire; De Boeck: Bruxelles, 2004. © DE BOECK, 2004.)

by a change to pH.[1,10] A reduction in fluorescence is observed when the temperature rises. This observation can be explained by several mechanisms:

1. An increase in the conversion rate from electronic energy levels to vibrational energy levels
2. Transition from the excited singlet state to an upper triplet intersystem crossover state
3. Loss of the plane structure of the molecule
4. The dissociation of molecular complexes in line with temperature.

A rise in temperature, therefore, intensifies the Brownian motion of the molecules. The frequency of collisions between molecules in the fluorophore and solvent increases, the dissipation of energy in the form of heat due to molecular motion and molecular shocks becomes very efficient, and the probability of a deactivation of internal conversion increases. The probability increases that the electronic state will change from singlet to triplet level. Incident radiation is not only absorbed or transmitted by the sample, it is also diffused in all directions. As the temperature of the medium rises, the

Encyclopedia of Analytical Chemistry, Online © 2006–2018 John Wiley & Sons, Ltd.

This article was published in the *Encyclopedia of Analytical Chemistry* in 2018 by John Wiley & Sons, Ltd.
DOI: 10.1002/9780470027318.a9540

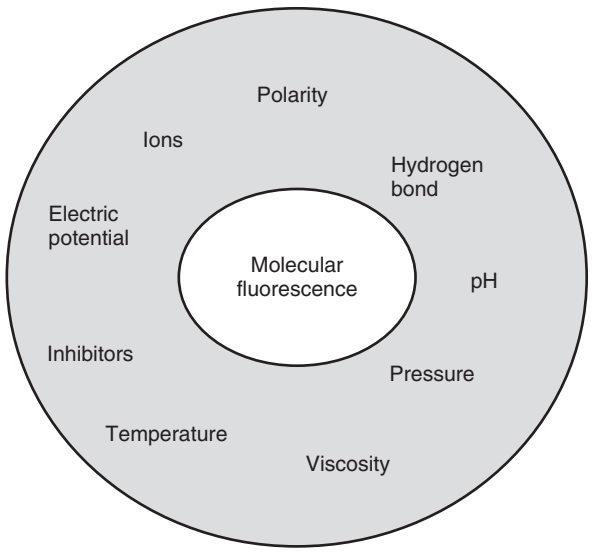

Figure 10 Schema of environment conditions. (Reproduced with permission from Valeur, B.: Invitation à la fluorescence moléculaire; De Boeck: Bruxelles, 2004. © DE BOECK, 2004.[1])

three parameters of fluorescence: intensity, quantum yield, and lifetime decrease. Ultimately, the temperature may also induce an extinction of the emission. The rise in quantum yield in line with pressure originates from vibrational relaxation processes at singlet-excited levels. The increase in the intersystem-crossing rate is due to an increase in the vibrational energy of singlet-excited levels. When pressure increases, vibrational relaxation processes induce intermolecular collisions, accelerate the transition from the initial vibrational level to vibrational states of lower energy. A reduction in fluorescence intensity is also observed.

Viscosity may also affect the intensity of fluorescence emission. An increase in fluorescence is observed when viscosity rises.[10] For example, a failure to take account of superimposed effects of nonindependent factors such as viscosity and temperature may lead to misinterpretation.[8] Decay of the fluorescence intensity of trans-stilbene is temperature-dependent, but not dependent on viscosity; it becomes isomerized in the excited state from the *cis* to the *trans* form.[8] It should also be noted that because UV light is used for excitation, photochemical decomposition may occur, with a decrease or even suppression of fluorescence.[10]

3.3 Diffusion

Light scattering is a phenomenon that can disrupt the fluorescence signal measured. This is the case with a weak Stokes shift, resulting in an overlap between the light scattering phenomenon and the emission peak of fluorophores (Figures 11 and 12). The scattering observed involves two light–matter interactions: Rayleigh and Raman scattering.

3.3.1 Rayleigh Scattering

Rayleigh scattering is a wave–matter interaction due to an elastic collision between a photon and electrons in the molecule. It involves the scattering of photons by electrons, which are much smaller than the incident wavelength. Photons are scattered not by free electrons but by those bound to an atom or molecule. The electric field of the incident wave deforms the electron cloud of the atoms; the center of gravity of the negative charges thus oscillates with respect to the positive charge of the nucleus. A dipole is thus created and radiates, causing induced radiation called Rayleigh scattering. The Rayleigh law states that the intensity diffused by a medium is inversely proportional to the fourth power of the wavelength of the incident light $1/\lambda^4$. In other words, the lower the wavelength the more the radiation will be scattered and the intensity of the scattered light will be higher. Wavelengths in the ultraviolet range are diffused more and therefore transmitted less than those in the infrared spectrum. Photons are scattered when the emission wavelength is the same as the excitation wavelength. There is no energy loss. Rayleigh scattering, therefore, does not carry chemical information on the medium under analysis and can disturb the fluorescence of compounds of interest by limiting sensitivity, particularly for wavelengths close to the excitation wavelength. It may be considered as an artifact, which needs to be removed in order to access the fluorescence signal of targeted molecules (Figure 11). In many cases, therefore, Rayleigh scattering may be of no interest to the chemical analysis because it is not linked to the concentration of molecules making up the sample. However, the shift between excitation and emission, as imposed by the Stokes' law, minimizes the risk of overlap with the emission spectrum of fluorophores. Rayleigh scattering is always visible when recording a 3D spectrum. Different methods are available to prevent its acquisition or enable its elimination during post-acquisition treatment.[20,21]

3.3.2 Raman Scattering

Raman scattering is also an interaction between photons arising from a monochromatic light source and molecules in the sample. Some photons at $1/10^8$ will be scattered inelastically with a slight loss of energy that corresponds to vibrational transition. Raman scattering occurs when the exciter electric field induces a change to

Encyclopedia of Analytical Chemistry, Online © 2006–2018 John Wiley & Sons, Ltd.

This article was published in the *Encyclopedia of Analytical Chemistry* in 2018 by John Wiley & Sons, Ltd.
DOI: 10.1002/9780470027318.a9540

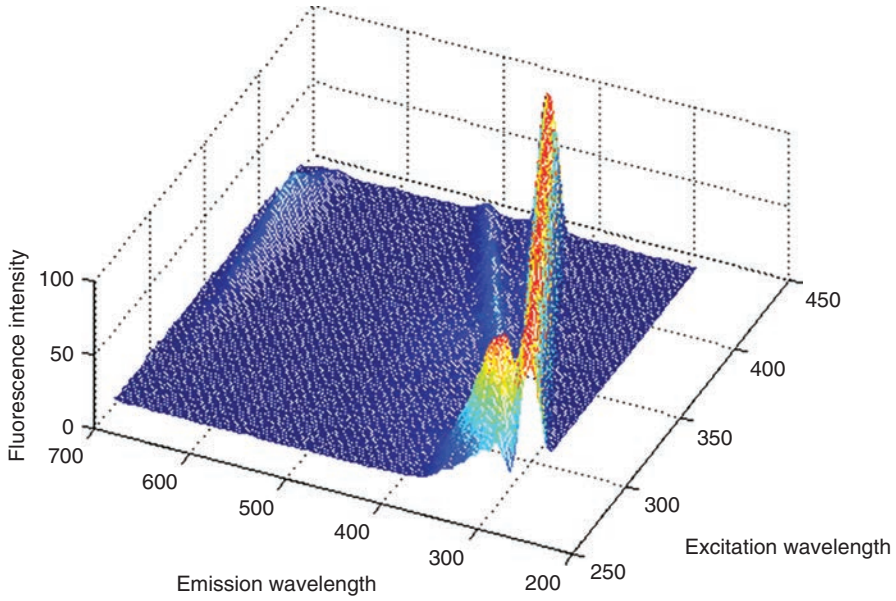

Figure 11 An example of 3D spectra of olive oil with Rayleigh scatter first order and Raman scatter.

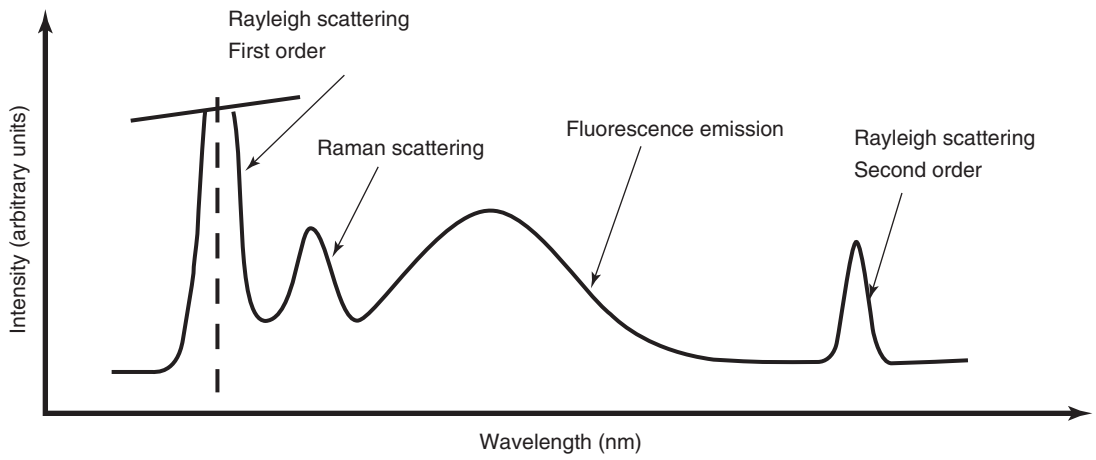

Figure 12 Schematic representation of scattering and fluorescence.

the polarization of the molecule. It can be particularly effective in detecting polarization changes during the vibration of homo- or heteronuclear skeletons. The result is a weak emission that may interfere or be confused with the fluorescence of the sample that is 100 to 1000 times weaker than Rayleigh scattering. Raman scattering does not mask the fluorescence signal, but its position may cause significant signal distortion.[22,23] Exploitation of the Raman interaction as a featuring signal of the molecules led to the development of Raman spectroscopy. This technology complements infrared spectroscopy. The former concerns variations in the polarization of chemical bonds, i.e. the dipole moment induces bonds while the second concerns the permanent dipole moment of the chemical bonds. Light–matter interaction processes cause particular vibrations to become active in either Infrared or Raman spectroscopy or both (mutual exclusion rules).

The applications of Raman spectroscopy may concern the determination of chemical structure, molecular configuration (cis, trans for polymers), the conformation of molecular arrangements (e.g. proteins in a helix or sheet, etc.), the study of molecular orientation, or intra and intermolecular forces.

Encyclopedia of Analytical Chemistry, Online © 2006–2018 John Wiley & Sons, Ltd.

This article was published in the *Encyclopedia of Analytical Chemistry* in 2018 by John Wiley & Sons, Ltd.
DOI: 10.1002/9780470027318.a9540

4 ANALYSIS OF FLUORESCENCE DATA

4.1 Structure of Fluorescence Data

According to Christensen,[15] 'an ideal fluorescence measurement device requires different conditions: 1. In order to obtain the most linear fluorescence intensity, the concentration range of the fluorophores must be sufficiently low; 2. For each fluorophore, the independence of fluorescence signals from each other is essential; 3. Compared to relevant fluorescence signals, signals from interfering species should be negligible. It is difficult for all these conditions to be met in real samples.' Given the complexity of the spectra, its use in targeted analysis is quite unusual; the spectra tend to be used as spectral fingerprints of samples. Data from the spectra can be used either quantitatively by linking the signals to fluorophore concentrations according to a calibration procedure, or under a fingerprinting approach that uses chemometrics and a greater number of observations to enable more efficient modeling. The multidimensional fluorescence signals recorded for a sample are presented in a fluorescence intensity matrix. This matrix is conventionally represented in a figure in plan view where color scale indicates the intensity and the abscissa and ordinate the excitation and emission wavelengths, respectively, as shown in Figure 4. This EEM for each fluorophore can be described as a function of a concentration-dependent factor $\boldsymbol{\alpha}$, its excitation $\boldsymbol{b}$ and emission characteristics $\boldsymbol{c}$. Overall fluorescence responds to the following equation[15]:

$$\text{EEM} = \sum_{i=1}^{n} \boldsymbol{\alpha}_i \times \boldsymbol{b}_i(\lambda_{ex}) \times \boldsymbol{c}_i(\lambda_{em}) \qquad (1)$$

Equation 1: Mathematical modeling of EEM.

To draw benefits from 3D fluorescence spectra, chemometrics is often used to extract interpretable information from these complex data. Chemometrics can be defined as the discipline that combines data analysis and analytical chemistry.[24] It gathers and develops a set of mathematical tools that can be used to extract structured and interpretable information from chemical data. Unlike statistics, chemometrics require few assumptions but need parameterization that governs the performance of the method. The validation step is, therefore, very important in chemometrics. Each sample produces an EEM matrix. Multiple matrices are combined to create a 3-way array cube, and if EEM are acquired under multiple experimental conditions, the data are arranged in an N-way array. This 3- or N-way array can then be used as input for two types of chemometric methods depending on whether its dimensions are kept intact or if it is unfolded in one or more chosen dimensions. In the former, it will be broken down using multiway or multimode methods such as parallel factors analysis (PARAFAC)[25] for 3-order tensors, or Tucker3 for N-order tensors. In the latter case, it will be analyzed in its unfolded form using 2-way algorithms from the same family as principal component analysis (PCA) (Figure 13).

4.2 The Chemometric Techniques Most Widely Used for Excitation Emission Matrix Data

3D fluorescence tends to be used for qualitative analysis, i.e. the data acquired by fluorescence spectroscopy are global for a sample without specifically orienting the analysis toward a particular chemical compound. This is called fingerprint analysis. This approach requires the use of chemometrics. However, there are cases where 3D fluorescence can enable quantification, particularly in the case of contaminants (Section 5.2), and the chemometric methods applied are different.

We can, therefore, make a distinction between unsupervised exploratory methods which enable a clearer understanding of the structure of the data, and supervised methods which use previously known complementary information on the data in order to model and predict the state of the system. This mainly concerns classification methods. In the case of unsupervised methods, the fluorescence intensity matrices are analyzed using techniques

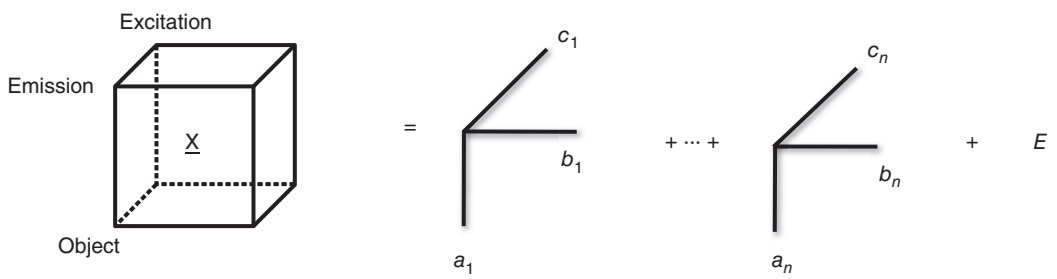

Figure 13 Principle of decomposition of a 3D cube according to the PARAFAC model.

Encyclopedia of Analytical Chemistry, Online © 2006–2018 John Wiley & Sons, Ltd.

This article was published in the *Encyclopedia of Analytical Chemistry* in 2018 by John Wiley & Sons, Ltd.
DOI: 10.1002/9780470027318.a9540

such as PCA, independent component analysis (ICA), or multivariate curve resolution-alternating least square (MCR-ALS). By construction, lines in the fluorescence matrices correspond to excitation wavelengths, while columns correspond to emission wavelengths. In most cases, a series of samples will produce a collection of excitation–emission matrices. This is arranged as a fluorescence cube that needs to be unfolded before PCA or ICA are applied.

PCA is the most widely known factorial method[26,27] It is of a multivariate exploratory nature that can reduce the dimensions of a dataset. It frequently employed as the basis for data compression techniques. It enables a representation of data in terms of the greatest variance in its main components.

ICA can be used to extract underlying signals from a mix of signals of unknown proportions and number.[28,29] ICA is, therefore, a technique for the blind separation of sources. Independent components (ICs) are calculated to be statistically independent of each other, the goal being to find physically significant vectors. Moreover, the optimum number of ICs is obtained using different techniques such as ICA-by-blocks or the Durbin–Watson criterion.[30–33] It is a powerful method in 3D fluorescence spectroscopy that can be used to identify chemically pure and therefore more interpretable signals.

MCR-ALS is a powerful modeling tool that can study complex chemical systems with a minimum number of assumptions and with flexibility on the constraints during profile optimization.[34–36] The objective of MCR-ALS is to recover chemically pure response patterns in the constituents or chemical species of an unresolved mixture from the information contained in the original dataset. In the case of 3D fluorescence spectra, and because the analysis is multiway, one of the most appropriate methods which respects the trilinear nature of fluorescence data is PARAFAC.

PARAFAC is a generalization of PCA to 3-higher order tensors.[37,38] The algorithm performs a trilinear decomposition, i.e. it breaks down the data cube into a sum of products of three vectors called PARAFAC loadings. These loadings form triplet vectors that contribute as far as possible to the evolution of signals according to the three multivariate directions that made up the initial cube. It is generally considered when analyzing fluorescence cubes that the vectors of the spectral modes form the basis for the decomposition of loadings, while the vectors of the first mode group the coordinate scores of the samples in the spectral base. In our case, the three modes are excitation wavelengths, emission wavelengths, and samples. PARAFAC is an efficient tool for the analysis of mixtures of several chemical compounds characterized by bilinear responses. PARAFAC can identify two profiles (the excitation profile and emission profile) of pure compounds and associate a proportion of them in the mixture. The model accepts constraints, the most common being nonnegativity and orthogonality.[39] In the case of EEM, only the nonnegativity constraint of loadings has a physical meaning. More information on this method is available elsewhere,[38,40] but also Rasmus Bro.[41–46] PARAFAC is also widely used in 3D fluorescence spectroscopy because it is mathematically very well suited to the trilinearity of the data. It is possible to work directly on the EEM and deduce pure signals.

When applying supervised methods, an initial data table calibration set is often available to build a model. This is then validated with another data set called the validation set.

One of the best-known methods is partial least squares (PLS) regression. This is a method used to construct predictive models when the factors are numerous and highly collinear. It enables the establishment of links between a set of dependent variables Y and a set of independent variables X when the number of variables (both independent and dependent) is high.[47] The result of the PLS is thus a set of matrices, which can be used to compute a series of regression coefficients B in order to predict new samples. Other supervised methods are also available, such as the support vector machine (SVM), discriminant factor analysis (DFA), or partial least squares-discriminant analysis (PLS-DA).

So depending on the purpose of the study, an unsupervised or supervised method will be chosen. However, some studies combine both approaches; there data are first of all processed using an exploratory method before a supervised method is applied.

5 THE PRINCIPAL NATURAL FLUOROPHORES

The use of 3D fluorescence enables the detection of different fluorophores present in samples. Because the total fluorophore composition of the sample is unknown, a 3D spectrum over a wide range of excitation and emission wavelengths makes it possible to obtain a spectral fingerprint of the sample. The use of chemometric methods provides the means to identify the fluorophores from pairs of excitation and emission wavelengths. It is nevertheless important to remember that in complex samples such as foods, fluorophore signals undergo environment-related interactions, which can lead to changes in the positions of the excitation–emission bands of fluorophores, thus rendering their identification more difficult.

In this section, we will be focusing on the identification of endogenous fluorophores in foods, water, soil, or

Encyclopedia of Analytical Chemistry, Online © 2006–2018 John Wiley & Sons, Ltd.

This article was published in the *Encyclopedia of Analytical Chemistry* in 2018 by John Wiley & Sons, Ltd.
DOI: 10.1002/9780470027318.a9540

biological fluids such as urine, and some examples will be detailed. In addition, a section will be devoted to exogenous fluorophores such as the contaminants that may also be detected in many matrices.

5.1 Endogenous Fluorophores

These are the fluorophores that are present naturally in the samples to be analyzed. These molecules may be aromatic amino acids, e.g. tryptophan, purines, pyrimidines, flavins, chlorophyll, certain enzymatic cofactors (e.g. NADH), riboflavin, and also numerous vitamins such as vitamins A, B, and E, as well as polyphenols.

5.1.1 Identification of Fluorophores in Foods

The principal difficulty associated with identifying fluorophores in food matrices which are by nature complex mixtures is the superimposition of signals of all the fluorophores present in the sample. It is, therefore, imperative to have chemometric tools capable of extracting the different signals that make up the fluorescence masses recorded. The identification process does not, therefore, involve the use of a large database of fluorophores constructed in various situations. Knowledge of the signals emitted by the most common fluorophores in various molecular environments is crucial to a good interpretation of the fluorescence data.[15,48] Figure 14 shows the standardized spectra of some fluorophores commonly found in foods.[15] These include vitamin E (λ_{ex} = 298 nm / λ_{em} = 325 nm), vitamin B2 – Riboflavin (λ_{ex} = 270 nm, 380 nm, 450 nm / λ_{em} = 520 nm), tryptophan (λ_{ex} 250–300 nm / λ_{em} = 280–350 nm), porphyrins such as chlorophyll (λ_{ex} = 420 nm / λ_{em} = 680 nm) and other molecules such as ATP (adenosine triphosphate – λ_{ex} = 292 nm / λ_{em} = 388 nm) and NAD (nicotinamide adenine dinucleotide – λ_{ex} = 344 nm / λ_{em} = 465 nm). A more exhaustive list of excitation and emission wavelengths useful for studying foods can be found in the FoodFluor database, which also offers access to excitation/emission couples used to obtain the specific spectral signatures of certain foods.[49] Airado-Rodriguez et al.[50] tried to identify families of fluorophores present in wine (Figure 15). The EEM matrices of several polyphenols characteristic of wine such, as flavan-3-ols (λ_{ex} = 280/ λ_{em} = 320–360 nm), catechin, and stilbenes (λ_{ex} = 318 nm / λ_{em} = 390 nm) such as resveratrol, were recorded. An equivalent study conducted on 50 air-dried medicinal herbs demonstrated the potential of 3D fluorescence spectroscopy coupled with the chemometric

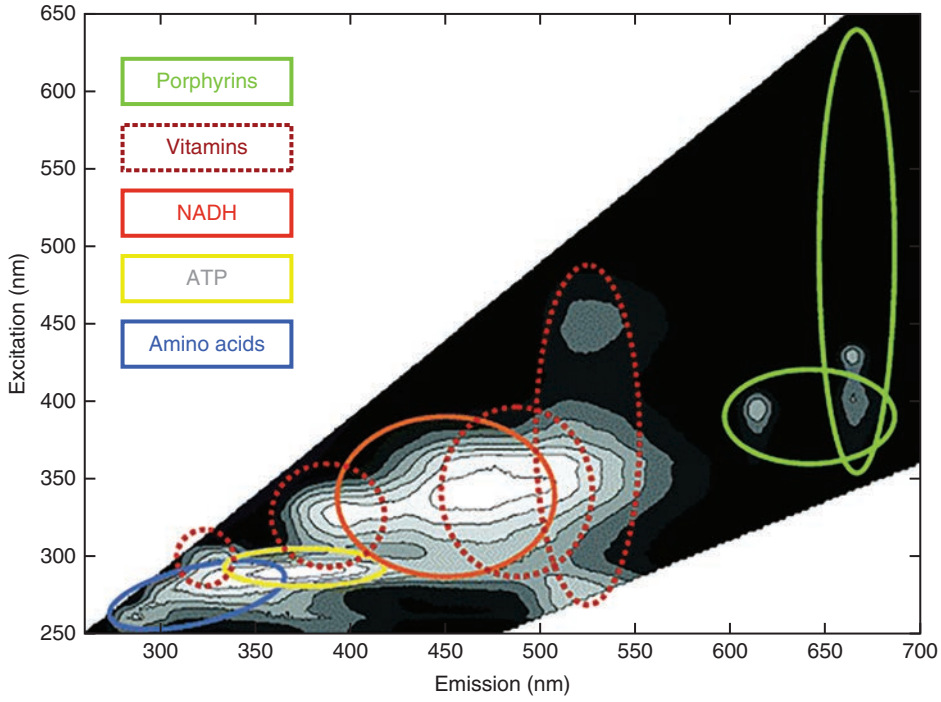

Figure 14 Fluorescence landscape map indicating the spectral properties of the selected 11 food-relevant fluorophores listed. (Reprinted with permission from Christensen J., Norgaard L., Bro R. and Engelsen S.r.B., Multivariate Autofluorescence of Intact Food Systems. Chemical Reviews, 106, 1979–1994 (2006). Copyright 2006 American Chemical Society.[15])

Encyclopedia of Analytical Chemistry, Online © 2006–2018 John Wiley & Sons, Ltd.

This article was published in the *Encyclopedia of Analytical Chemistry* in 2018 by John Wiley & Sons, Ltd.
DOI: 10.1002/9780470027318.a9540

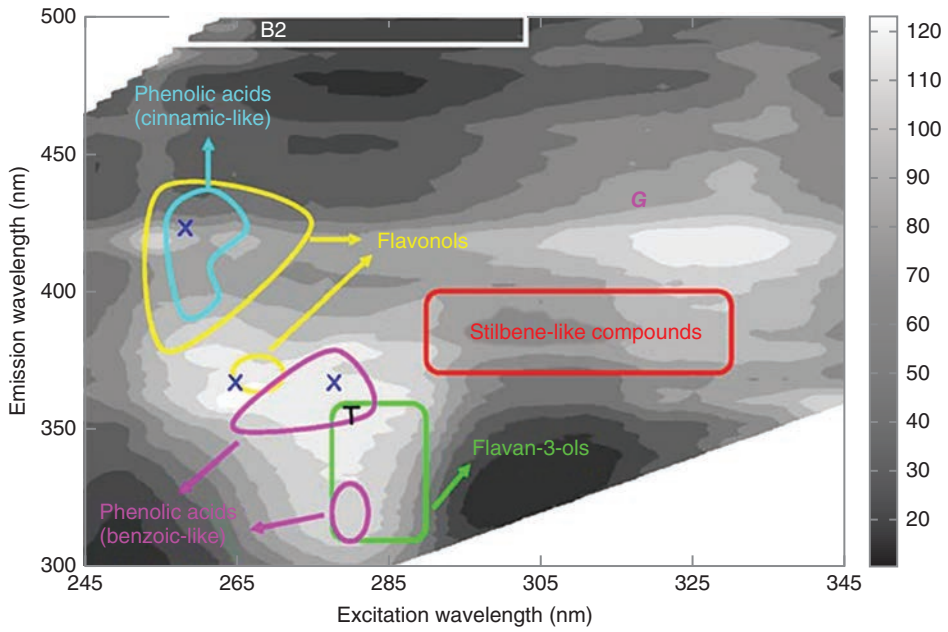

Figure 15 Fluorescence landscape corresponding to one of the wine samples included in this study, indicating the fluorescent properties of typical fluorophores of wine. (X: phenolic aldehydes; G: gentisic acid; T: tryptophan; B2: vitamin B2). Gray scale represents fluorescence intensity. (Reproduced with permission from Ref. 50. © Elsevier, 2011.)

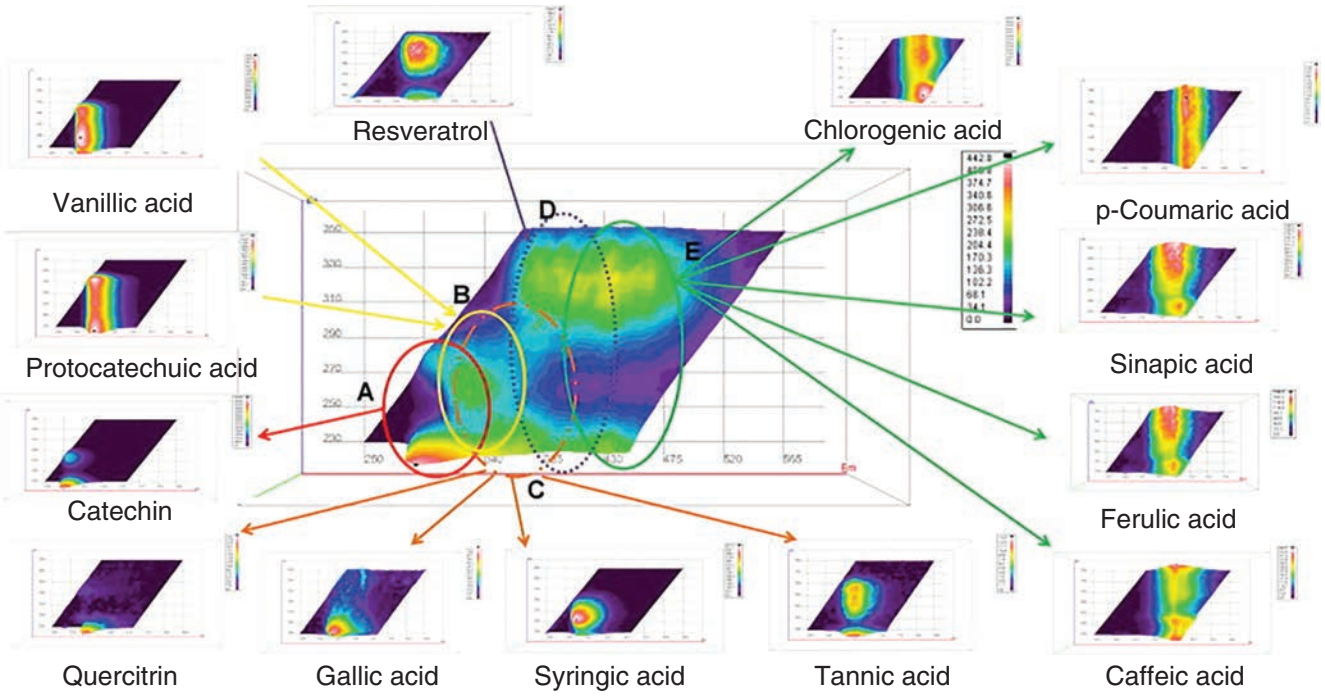

Figure 16 The fluorescence fingerprint corresponding to one of the HM extracts in methanol (S51), indicating the fluorescent properties of typical fluorophores of HM. (Reproduced with permission from Ref. 51. © Elsevier, 2015.)

Encyclopedia of Analytical Chemistry, Online © 2006–2018 John Wiley & Sons, Ltd.

This article was published in the *Encyclopedia of Analytical Chemistry* in 2018 by John Wiley & Sons, Ltd.
DOI: 10.1002/9780470027318.a9540

methods PARAFAC-PCA/CA to identify 13 polyphenols (Figure 16).[51] Many studies have been performed to characterize foods using 3D fluorescence spectroscopy. Table 1 shows examples of such foods, with the name of the food matrix, the purpose of the study, the excitation and emission wavelength ranges, the fluorophores studied, the chemometric treatment, the results obtained, and bibliographical references.

5.1.2 Fluorophores in the Environment

Dissolved organic matter (DOM) and its fluctuations are an essential element in the quality of terrestrial and aquatic natural systems, so its study is crucial. In this field, 3D fluorescence spectroscopy coupled with chemometrics can produce very promising results when characterizing DOM in different freshwater, marine, and soil environments.[75,76] The number of publications in this area is considerable, so we have chosen to present the main features of DOM based on the papers by Ishii and Boyer,[77] Henderson et al.,[78] Bridgeman et al.,[79] Carstea et al.,[80] and Yang et al.[81] and some articles from teams who have done a lot of work in this field such as Coble,[82] Stedmon et al.,[83–87] and Chen et al.[88]

General remark: One of the problems encountered when exploiting 3D fluorescence signals is linked to the fact that a fluorescence intensity may be the combination of several fluorescence emissions from different fluorophores responding to the same excitation–emission pair. A fluorescence mass is then obtained whose envelope is the weighted sum of several underlying signals. One possible solution is to try to estimate the contribution of each of the signals making up the fluorescent signal, as proposed in the fluorescence regional integration (FRI) method.[88] The originality of this method is that it enables the quantification of several EEM peaks. Quantitative analysis using the FRI technique is based on integrating the volume below each region of the EEM spectrum. It is thus possible to specify zones with excitation and emission wavelengths that correspond to a particular fluorophore. Integration of the bands observed in a given region of the EEM can be performed under the reasonable assumption that the fluorescence signal represents the cumulative fluorescence response of all DOM present in the sample. Figure 17 shows the fluorescence regions characteristic of organic matter. It has been shown that molecular families are found in fairly well-delimited regions, thus facilitating their

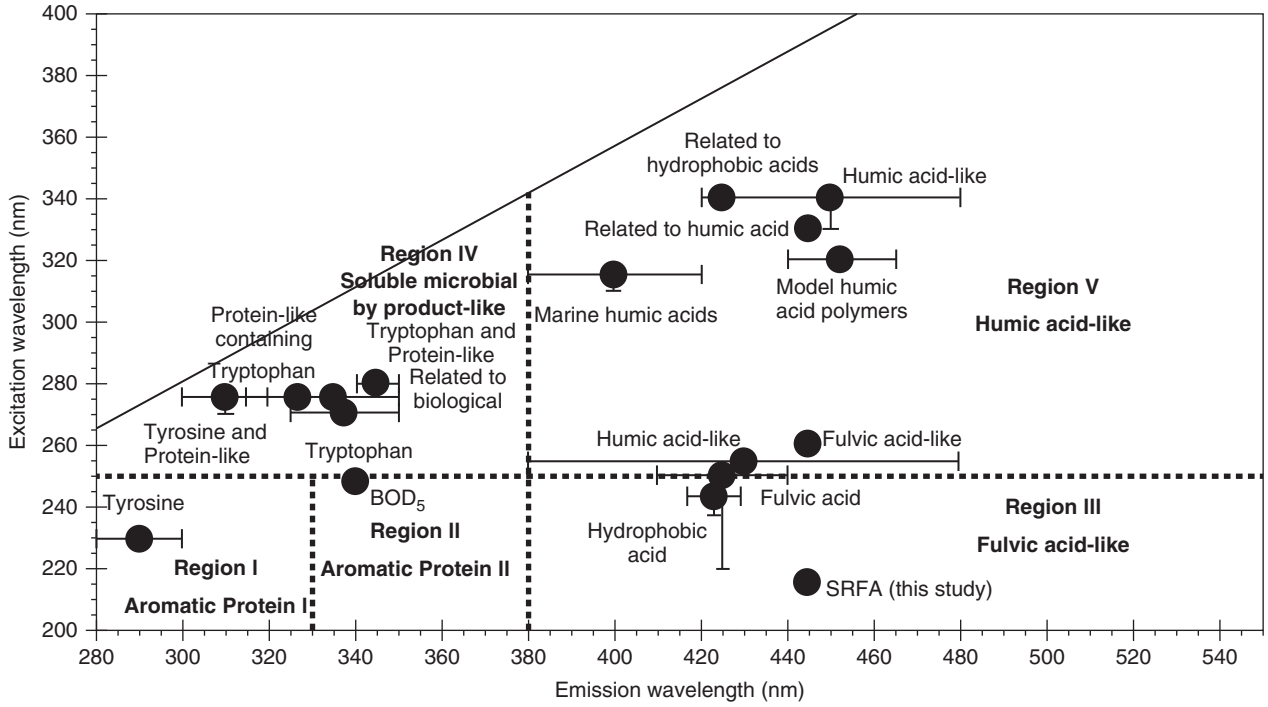

Figure 17 Location of EEM peaks (symbols) based on literature reports and operationally defined excitation and emission wavelength boundaries (dashed lines) for five EEM regions. (Reprinted with permission from Chen, W.; Westerhoff, P.; Leenheer, J. A.; Booksh, K.: Fluorescence Excitation-Emission Matrix Regional Integration to Quantify Spectra for Dissolved Organic Matter. Environmental Science & Technology 2003, 37, 5701–5710. Copyright 2003 American Chemical Society.[88])

Encyclopedia of Analytical Chemistry, Online © 2006–2018 John Wiley & Sons, Ltd.

This article was published in the *Encyclopedia of Analytical Chemistry* in 2018 by John Wiley & Sons, Ltd.
DOI: 10.1002/9780470027318.a9540

Table 1 Recapitulation of articles concerning food samples using EEM or synchronous fluorescence spectra

Food products	Objectives	Method	λ_{ex} (nm)	λ_{em} (nm)	Fluorophore	Chemometric treatment	References
Apple juice	To evaluate the quality of apple juice Discrimination of quality grade. See Section 6.2	EEM	230–350	250–565	Polyphenols	PCA kNN classification	52
Apple juice	To investigate the feasibility of synchronous fluorescence and chemometrics for screening antioxidant properties	FF SFS	240–700	$\Delta\lambda$ =10–160	Polyphenols Flavonoids	PCA PLS	53
Beef	To predict the aerobic plate count (APC) on the surface of beef using fluorescence fingerprinting	EEM	200–900	200–900	Trp NADPH Porphyrin	PLS	54
Carrot-based baby food Carrot puree	To evaluate 3D-FFFS to monitor the impact of industrial processes on carrot-based baby foods To calibrate neoformed compounds (NFC). See Section 6.3	EEM	208–512	280–712	Trp Vitamin E Polyphenols Maillard reaction Vitamin B2 Porphyrins	PARAFAC	55
Cheese	To show that fluorescence provides information on several parameters involved in lipid oxidation. See Section 6.2	EEM	260–360 360–460	280–600 390–650	Trp Tyr Vit A retinol B carotene Riboflavin	PARAFAC	56
Cheese	To use multivariate analysis on 3D-FFFS to obtain data on of age and storage conditions in cheese. See Section 6.2	EEM	240–360 Δ = 20 nm	275–475	Trp Maillard products Vitamin A	PARAFAC	57
Cheese	To investigate the impact of NaCl reduction and its substitution with KCl	SFS	250–550	$\Delta\lambda$ = 20, 40, 60, 80, 100, 120	Trp Riboflavin NADH FADH Maillard products	ICA	58
Cookies	To evaluate the potential of using 3D-FFFS for the rapid quantitative estimation of neoformed contaminants in industrially processed cookies. See Section 6.3	SFS	280–550	$\Delta\lambda$ = 0–140	Trp Nf Riboflavin	PARAFAC	13
Fruit spirits	To distinguish between spirit types by applying DA to the SFS of spirits Classification. See Section 6.1	EEM	EX 200–500 SFS 200–600	EM 250–600 Offset 10–100	Guaiacol Eugenol Phenylethanol Polyphenols	PCA LDA GDA	59
Honey	To characterize honey samples and build a model for classification. See Section 6.1	EEM	240–500	270–640		PARAFAC PLS-DA	60
Honey	To characterize honey	RA EEM	260–400	300–600	Trp Polyphenols	PCA LDA	61
Meat	To detect the principal fluorophores in meat and the effects of cooking kinetics (3D-FFFS). See Section 6.3	SFS	250–550	Offset 20–160	Trp Maillard products Heterocyclic aromatic amines	PCA PARAFAC	62

Encyclopedia of Analytical Chemistry, Online © 2006–2018 John Wiley & Sons, Ltd.

This article was published in the *Encyclopedia of Analytical Chemistry* in 2018 by John Wiley & Sons, Ltd.
DOI: 10.1002/9780470027318.a9540

Milk fat	To detect the adulteration of milk with vegetable oils	EEM	250 550	310 700	Trp Riboflavin	PCA	63
Milk: skimmed and raw	To characterize the heat treatment of milk performed using instant infusion pasteurization. See Section 6.3	EEM	250–330 330–350	260–360 nm 260–500 nm	Trp	PARAFAC	64
Nuts and seeds	To explore the potential of 3D-FFFS data analysis to predict quality parameters related to lipid-rich foods such as nuts and seeds. See Section 6.3	EEM	280–600	280–700	Trp Maillard products	PARAFAC	65
Edible oils	To develop a classification of different edible oils during heating using synchronous fluorescence spectra. See Section 6.1	SFS	250–720	Offset 20–120 with		PCA	66
Olive oil	To demonstrate the potential of 3D-FFFS and 3-way PARAFAC and N-PLS methods to characterize olive oil. See Section 6.1	EEM	300–390	415–600		PARAFAC	67
Olive oils	Test cluster analysis to discriminate three main types of olive oil. See Section 6.1	EEM	300–400	400–700	Chlorophyll Oxidation products	HAC	68
Vegetable oils and Nigella sativa	To demonstrate the usefulness of ICA as a means to extract pure underlying signals from a set of mixed signals with unknown proportions. See Section 6.3	EEM	280–500	300–550	Tocopherol Oxidation products	ICA	69
Virgin olive oil thermoxidized (VOO)	To propose 3D-FFFS combined with PARAFAC as a tool to monitor fluorescence changes to VOO. Process changes. See Section 6.3	EEM	250–298	300–700	Tocopherols Oxidation products Chlorophyll	PARAFAC	70
Shrimps	Geographical classification of shrimps. See Section 6.1	EEM	230–600	240–600		PARAFAC SIMCA	71
Wines	EEM + PARAFAC can distinguish between wine samples from different appellations and obtained using different aging processes. See Section 6.1	EEM	245–345	300–500	Polyphenols	Pretreatment remove Rayleigh signals PARAFAC	50
White wines	To classify white wines according to grape variety. See Section 6.1	EEM	245–341	375–500		SIMCA PARAFAC N-PLS-DA U-PLS-DA	72
Yogurt	To demonstrate that 3D-FFFS and chemometrics can be used to monitor light-induced changes in plain yogurt during storage. See Section 6.3	EEM	270–550	310–590	Riboflavin	PCA PLSR	73
Bread dough	To study the influence of formulation and duration of mixing in bread dough using front-face 3D-FFFS and ICA	EEM	240–400	250–500	Trp Ferulic acid	PCA ICA	74

HAC, hierarchical agglomerative clustering; LDA, linear discriminant analysis; FF SFS, front face synchronous fluorescence spectroscopy; FFFS, front face fluorescence spectroscopy; RA, right angle; Trp : Tryptophane.

Encyclopedia of Analytical Chemistry, Online © 2006–2018 John Wiley & Sons, Ltd.

This article was published in the *Encyclopedia of Analytical Chemistry* in 2018 by John Wiley & Sons, Ltd.
DOI: 10.1002/9780470027318.a9540

identification. For example, regions I and II correspond to aromatic proteins such as tyrosine; region IV is that of soluble microbial by-products, whereas region V is associated with humic acids. Finally, region III, which corresponds to excitation wavelengths <250 nm and emission wavelengths >350 nm, is associated with molecules such as fulvic acid. Figure 17 groups several families of fluorophores that might be found in environmental samples, including soil. Because the FRI method is reliant on integrating the volume below each region, its use remains limited when there is spectral interference or if one spectrum conceals another. An alternative to the FRI method is PARAFAC. Indeed, a study presenting a PARAFAC model with six components[89] showed that it is possible to link PARAFAC loadings to different components of marine ecosystems, soils, water, proteins, humic acids, etc. This work provided elements for interpreting fluorescence data and specified the location of useful fluorescence signals on EEMs (Table 2). PARAFAC thus makes it possible to characterize each component of DOM in the environment. It is generally reported that component 1 corresponds to the group of humic fluorophores that can characterize terrestrial environments such as soils, whereas component 2 is more closely related to quinone-like compounds[90] and tends to be used to characterize aquatic environments.[84–87] Component 3, more variable in the studies, can be used for both terrestrial and aquatic environments as it is linked to high concentrations of chlorophyll. If the components are compared with the regions, it can be seen that component 3 has the closest correspondence to region IV.[88] In the case of wastewater component 1 is absent, but it appears and increases with precipitation due to runoff.[84] Components 2 and 3 enable a clearer characterization of wastewater. Component 2 is important in treated water.[91,92] On the other hand, component 3 is an excellent indicator of sewage contamination in swimming pools.[93] With respect to light, component 1 is more highly concentrated on the surface of water so it is more resistant to photodegradation, whereas component 2 is found at higher levels in groundwater and is, therefore, more sensitive to photodegradation.[87,94] Component 3 is intermediate in terms of its weaker sensitivity to photodegradation.

The majority of PARAFAC studies have attempted to describe temporal and spatial variabilities of DOM. But to date, it has not been confirmed whether variations in DOM fluorescence are due to chemical transformation, physical transformation, or modifications to the source of DOM. Table 3 presents the technical aspects of the main articles cited here. For a general overview, many of the studies performed on DOM since the 2000s, in particular, were summarized and criticized in the review by Ishii and Boyer.[77]

5.1.3 Fluorophores in Other Media

Although most of the literature concerns the environment and foods, a number of preliminary studies have been performed in biological media. Studies on urine, blood, or plasma samples were carried out in order to make a distinction between malignant and healthy cells[100–102] or to achieve a rapid diagnosis of urinary tract infection[103] (Section 6.2). A study on a new method for the kinetic and quantitative analysis of NADH degradation and FAD formation in plasma[104] is also worthy of mention. Anecdotally, the literature reports particular studies on the analysis of butterfly wings,[105] pollen,[106] and also works of art.[107] Some examples are shown in Table 4.

5.2 Exogenous Fluorophores

Exogenous fluorophores are the fluorescent compounds contained in a matrix – whether it be food, water, soil, animals, or plants – but which did not initially belong to this matrix (Table 5). These are external pollutants such as drugs or contaminants. The emission of fluorescence is strongly influenced by the medium, and fluorescent molecules can be used to label a target molecule, being referred to as fluorescent probes; however, we will not be focusing on them in this article but readers can find detailed aspects concerning them elsewhere.[1] Exogenous fluorophores include contaminants such as polycyclic aromatic hydrocarbons (PAHs), pesticides, aromatic amines, and also mycotoxins and drugs, etc. For PAH and pesticides, conventional tests such as chromatographic methods are effective but extremely time-consuming and laborious. For these reasons, 3D fluorescence spectroscopy is preferred, although there may sometimes be a more or less significant overlap between the excitation and emission bands of PAHs and other interfering compounds, which can lead to a lack of selectivity. This problem can partly be solved through the use of chemometric methods, on the one hand, to deconvolute the signal and quantify these compounds individually. A study[108] was thus published using 3D fluorescence analysis combined with PARAFAC to discriminate and quantify certain PAHs and pesticides such as dimethyl naphthalene, fluorene, phenanthrene, anthracene, pyrene, benzo[a]anthracene, and pesticides at concentrations of around microgram per liter and in the presence of humic substances. Inhibition phenomena affecting PAHs and pesticides may occur when concentrations of humic substances exceed 2.5 mg L^{-1}. When comparing the results concerning PARAFAC components from fluorescence analysis, PAH concentrations obtained using GC-MS with natural samples, the correlation varies as a function of the PAHs and is much better for alkylated PAHs ($r^2 = 0.9$). Fluorescence spectroscopy

Encyclopedia of Analytical Chemistry, Online © 2006–2018 John Wiley & Sons, Ltd.

This article was published in the *Encyclopedia of Analytical Chemistry* in 2018 by John Wiley & Sons, Ltd.
DOI: 10.1002/9780470027318.a9540

Table 2 EEM locations, representative EEMs, and spectral loadings for reoccurring PARAFAC components; excitation curves in spectral loadings are to the left of emission curves

Component Label (this study)	Approximate EEM location	EEM	Spectral Loadings
1	Ex: <230-260 nm Em: 400-500 nm	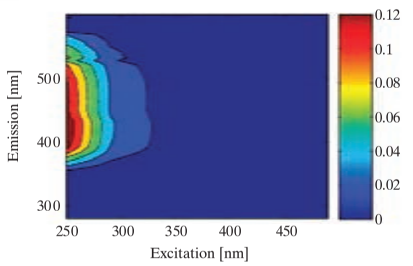	
2	Ex: <240-275(339-420)[1] nm Em: 434-520 nm	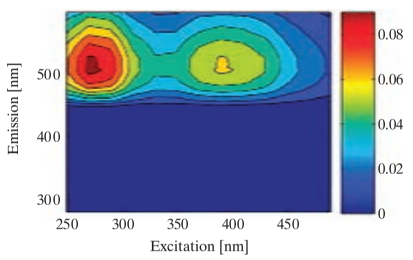	
3	Ex: <240-260(295-380)[1] nm Em: 374-450 nm	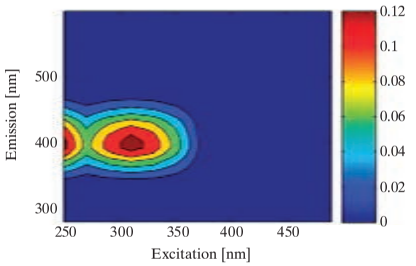	

Reproduced with permission from Ref. 89. © Elsevier, 2009.

Encyclopedia of Analytical Chemistry. Online © 2006–2018 John Wiley & Sons, Ltd.

This article was published in the *Encyclopedia of Analytical Chemistry* in 2018 by John Wiley & Sons, Ltd.
DOI: 10.1002/9780470027318.a9540

Table 3 Some examples of fluorophores found in environmental samples (water, soil, etc.)

Matrix Samples	Aim	Excitation (nm)	Emission (nm)	Fluorophores	Chemometric treatment	References
Seawater	To examine the range of environmental variability in the fluorescence properties of naturally occurring DOM	260 455	270 510 465 709	Tyr-like Tryp-like Humic-like Marine humic-like		82
Reclaimed water samples Excess sludge sample	To predict the potential for the formation of disinfection by-products in recycled water. See Section 6.3	200–450	250–600	Humic acid (HA) Fulvic acid (FA)	Regression models	95
Water samples and wastewater samples	To use EEM as a fingerprinting tool to monitor wastewater systems. See Section 6.3	200–500	225–625	Humic acid BSA	PARAFAC	96
Asphaltene samples	To extract information from asphaltene samples at different concentrations using fluorescence spectroscopy with MCR-ALS. See Section 6.1	300 400	320 700	Monomer Dimer Trimer	MCR-ALS	97
Swimming pool water	To study the EEM of DOM in swimming pools to generate data on water quality	240 450	300 600	Humic-like	PARAFAC	93
Composts	To evaluate the application of solid sample phase (SPF)–EEM to organic matter in compost	250 500	300 600	Humic-like Protein-like	PARAFAC	75
Municipal recycled water treatment plants	To obtain a robust characterization of DOM using EEM in recycled municipal water plants	200 400	280 500	Terrestrial humic-like Microbial humic-like Protein-like	PARAFAC	92
Aquatic ecosystems	To trace fractions of DOM in aquatic systems using EEM	240 400	320 580	Humic-like Soil fulvic-like Protein-like	PARAFAC	86
DOM	To characterize organic matter in aqueous systems and tutorial	200 400	280 500	Humics (3) Tyrosine Tryptophan	PARAFAC NPLS SOM ANN	98, 99

can, therefore, be used as a low-cost screening method to monitor PAH and pesticide concentrations at microgram per liter levels in chronically or sporadically contaminated natural water. An improvement in the detection threshold of 3D fluorescence could be achieved with better sample preparation, a more sensitive fluorescence detector and/or a chemometric approach which could better deconvolute the fluorescence signal. One study[109] involved obtaining pesticide fluorescence fingerprints through their direct identification as target compounds in soil and water samples. The database used described 48 pesticides used in Morocco. The problem was to attain the limit of detection, particularly without sample preparation. This approach reported by Ferretto et al.[108] might be better suited to use as an alert method in the event of massive contamination by any fluorescent pollutant[109] rather than the accurate quantification of soil pollutants. In the papers described earlier, it appeared that 3D fluorescence could not generate positive results at the desired concentrations for the analysis of contaminants, i.e. at nanogram per liter. Elcoroaristizabal et al.[110] tested the MCR-ALS, PARAFAC, and U-PLS/RBL (unfolded partial least squares coupled to residual bilinearization) algorithms (Figure 18) and compared them in order to obtain qualitative and quantitative information on the analytes and their interferences in complex samples of PAH mixtures analyzed using EEM fluorescence spectroscopy.

Encyclopedia of Analytical Chemistry, Online © 2006–2018 John Wiley & Sons, Ltd.

This article was published in the *Encyclopedia of Analytical Chemistry* in 2018 by John Wiley & Sons, Ltd.
DOI: 10.1002/9780470027318.a9540

Table 4 Some examples of biological and other samples

Matrix	Aim	Excitation (nm)	Emission (nm)	Fluorophores	Chemometric treatment	References
Human blood plasma samples Diluted and undiluted	To explore EEM F as a potential metabonomic tool for the early detection of colorectal cancer	250–450	300–600	Tryp NADPH	PARAFAC	100
Breast cancer samples (38) 20× diluted 500× diluted	To discriminate breast cancer samples by measuring the fluorescence of serum samples (diluted and undiluted) combined with chemometric tools	230 400	250 600	Three tumor markers CA15-3, CEA, TPA	ECVA LDA	101
Mouse skin	To characterize the early diagnosis of neoplastic changes in DMBA-TPA-induced mouse skin carcinogenesis	280–460	300 700	Trp Collagen NADH FAD Porphyrin	DA	102
Urine samples	Using EEMF to develop a simple and rapid diagnostic tool for urinary tract infections	250 450 SFS	310 750 Offset 90 and 30	Tryp Indoxyl sulfate Indoxyl 3 acetate Xanthine		103
Butterflies	To classify different types of butterfly	200–400	300–500	Pteridine pigments		105
Pollens, proteins, standards (pollen powder, proteins, bacteria, spores, fungi)	To discriminate pollen among other bio-particles under lab conditions using fluorescence and FTIR	250–400	260–550		PCA	106
Components included in paintings	To classify selected resins, oils and protein-based media used in paintings	300–500	Offset 10–150		PCA HCA	107

ECVA, extended canonical variates analysis; LDA, linear discriminant analysis; DMBA-TPA, 7,12-dimethylbenz(a)anthracene/12-O-tetradecanoylphorbol-13-acetate; FTIR, Fourier transform infra red spectroscopy.

Table 5 Different sources of major contaminants

Major contaminants	Examples
Environmental contaminants	Polycyclic aromatic hydrocarbons, pesticides, mycotoxins
Food process contaminants	Acrylamide, Maillard products, aromatic amines
Unauthorized adulterants and food additives	See Section 6
Substances migrating from packaging materials	See Section 6.4
Veterinary or human medicinal products	Esoxacin

For screening purposes, the application of PARAFAC or MCR-ALS offers added value for the detection of unexpected compounds in a system and the ability to identify the most contaminated samples. In the latter case, a second step can involve U-PLS/RBL in order to accurately estimate the concentrations of analytes of interest. The results obtained can be compared with more expensive and time-consuming separation techniques such as HPLC-FLD. Figure 18 summarizes the different chemometric treatments that are available. The unfolded PLS method coupled with residual bilinearization (U-PLS/RBL)[110–112] is a multivariate calibration method. Its main objective is the optimal prediction of concentrations in a matrix Y using a model that links the concentrations with information from EEM fluorescence measurements in a matrix X. U-PLS is coupled with RBL to obtain a second-order benefit. RBL is a postcalibration procedure based on a PCA and can be used to model the presence of unexpected constituents in a sample. Unlike PARAFAC and MCR-ALS, where calibration and test samples are jointly broken down by the model, U-PLS/RBL does not include unknown samples at the calibration stage. Although U-PLS/RBL is more flexible, this also implies a non-unique solution.

Encyclopedia of Analytical Chemistry, Online © 2006–2018 John Wiley & Sons, Ltd.

This article was published in the *Encyclopedia of Analytical Chemistry* in 2018 by John Wiley & Sons, Ltd.
DOI: 10.1002/9780470027318.a9540

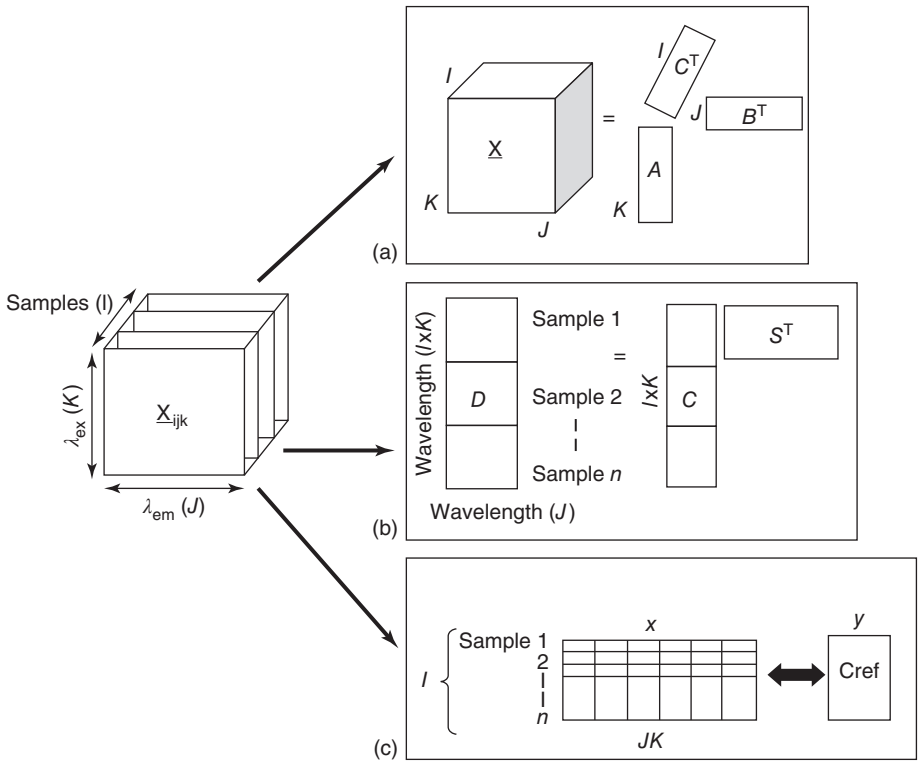

Figure 18 Graphical representation of the data structure employed in the second-order algorithms: PARAFAC (a), MCR–ALS (b), and U-PLS/RBL (c). (Reproduced with permission from Ref. 110. © Elsevier, 2014.)

To test the various algorithms, a calibration set of 49 standard solutions of 9 PAH, and then a validation set of 25 PAH solutions, were prepared. The interference study was carried out using two mixtures containing the 16 US-EPA PAHs. While PARAFAC and MCR-ALS required 11 factors to produce the best results with the calibration set, U-PLS required 10. For the validation set, 25 solutions are tested. Satisfactory predictions were obtained with better results for U-PLS. PARAFAC and MCR-ALS required a single model for all PAHs while U-PLS required one model for each PAH. It can thus be seen that PARAFAC and MCR-ALS are good algorithms which are appropriate for rapid qualitative and quantitative screening in environmental samples, but a compromise is still necessary between performance of the methods and the complexity of the results in terms of the models that need to be managed. U-PLS is a calibration method; it provides better quantitative information for samples involving interferences and a potential matrix effect. But it has two drawbacks: the estimation of the number of unexpected contributions at the RBL stage, and the enormous computation time required to build the models. The latter method could be used as a second step to accurately estimate the concentrations of analytes of interest. Table 6 describes technical information from recent articles related to EEMs and exogenous fluorophores. 3D fluorescence combined with chemometric tools can, therefore, be used to analyze contaminants such as PAHs, and also pesticides, mycotoxins, etc. The limiting factor of this technique is the limit of detection in some cases. It has been seen in two very different cases that by applying U-PLS/RBL after PARAFAC, it is possible to obtain more efficient quantitative results.

6 APPLICATIONS

The following synthesis will focus on describing applications as a function of the purpose of the analysis, based on different original articles that will be detailed regarding their analytical and chemometric approaches. It can be seen that analysis using 3D fluorescence spectroscopy is often untargeted and rather a fingerprint approach; the aim is mainly to characterize the samples in order to determine and highlight what differentiates them from a chemical point of view. For this purpose, the use of chemometrics is necessary or even mandatory.

Encyclopedia of Analytical Chemistry, Online © 2006–2018 John Wiley & Sons, Ltd.

This article was published in the *Encyclopedia of Analytical Chemistry* in 2018 by John Wiley & Sons, Ltd.
DOI: 10.1002/9780470027318.a9540

Table 6 List of papers related to contaminants using excitation–emission fluorescence spectroscopy

Matrix samples samples	Aim	Excitation (nm)	Emission (nm)	Fluorophores	Chemometric treatment	Other analysis	References
PAH In hexane	To develop a rapid and reliable method based on total fluorescence spectroscopy and the combined use of second order data analysis algorithms	240–320	290–550	PAH: Ant, Fluo, BaA, Chr, BbF, BkF, BaP, DahA, BghiP, IcdP and mixtures	PARAFAC MCR–ALS U-PLS/RBL		110
PAH Water samples	To characterize the fluorescence signatures of PAH and pesticides and discriminate using PARAFAC, applied to natural samples	200–500	280–550	Some PAH: Naph, DNaph, Flu, DFlu, Phe, BeP, Pestic: Pho, Car, Thi	PARAFAC	PAH extraction GC-MS analysis	108
PAH	To demonstrate the ability of single exposure EEM spectrofluorimetry to determine aqueous PAHs	230–290 260–319 210–270 280–340	270–430 378–490 295–455 370–530	BF BaP Phe BkF	PARAFAC		113
PAH Water samples	To determine simultaneous ultratraces of BaP and DBA in a highly interfering environment	250–367	380–480	BaP DBA	PARAFAC	Microscopic images SPE HPLC	114
Dried lime tree flowers Extract of lime flower, in a tea bag then diluted	To generalize the use of EEM to determine carbamate pesticides in matrices when a quenching effect exists	240–290	295–500	Carbamates: Carbaryl Carbendazim 1-Naphtol Quenching effect	PARAFAC		115
Mycotoxins	To quantify mycotoxins in cereal samples	250–400	400–500	Aflatoxin Ochratoxin A	PARAFAC N-PLS/RBL		116
Fluoroquinolones	To quantify different fluoroquinolones in urine samples using synchronous fluorescence spectroscopy	202–490	300–588	Pefloxacin Enoxacin Ofloxacin	NPLS and UPLS		117
Active pharmaceutical ingredients (APIs)	To evaluate the potential of fluorescence sensing to quantify two APIs simultaneously and nondestructively	280–365	300–500	Flupentixol (FLU) Melitracen (MEL)	PCA iPLS	Simultaneously quantification with 9 % error	118
Heterocyclic aromatic amines (HAA) in grilled meat	To determine HAA in grilled meat using synchronous fluorescence spectroscopy	250 550	Δλ 20–160	4–8 diMetQx MelQx IQ PhI	PARAFAC N-PLS	LC-APCI MS/MS	119
Sulphonamides in milk	To determine sulphonamide levels in different milk samples	350–450	420 550		PARAFAC PLS PLS–CM		120

PLS–CM, partial least square–class modelling.

Encyclopedia of Analytical Chemistry, Online © 2006–2018 John Wiley & Sons, Ltd.

This article was published in the *Encyclopedia of Analytical Chemistry* in 2018 by John Wiley & Sons, Ltd.
DOI: 10.1002/9780470027318.a9540

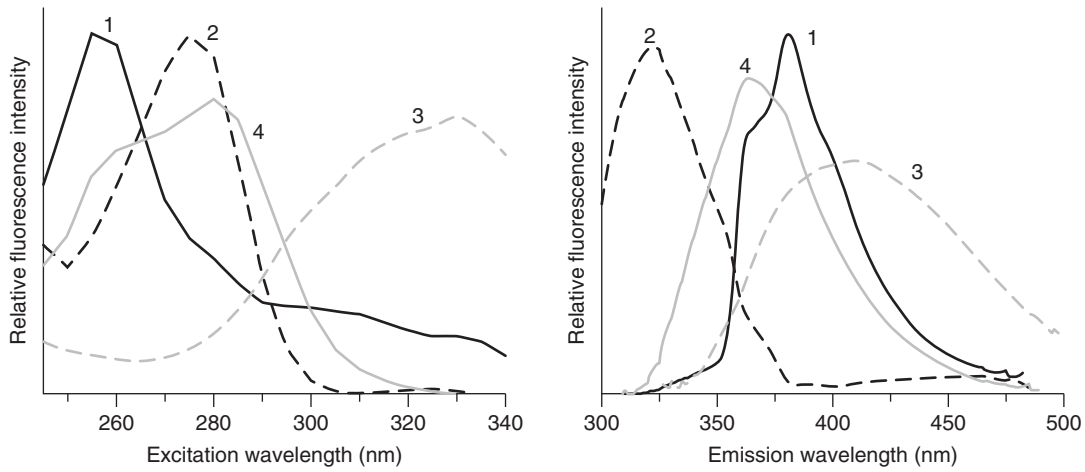

Figure 19 PARAFAC fluorescent loadings for the four components of the non-negativity constrained PARAFAC model constructed on the basis of the fluorescent landscapes of 57 wine samples. (Reprinted with permission from Airado-Rodriguez, D., Galeano-Diaz, T., Duran-Meras, I., and Wold, J. P. (2009). Usefulness of Fluorescence Excitation-Emission Matrices in Combination with PARAFAC, as Fingerprints of Red Wines. Journal of Agricultural and Food Chemistry 57, 1711–1720. Copyright 2009 American Chemical Society.[121])

This article will address the subject in terms of the objectives commonly encountered in the scientific literature: classification, authentication, discrimination, evaluation (particularly quality levels), the implementation of process indicators, and the detection of adulteration.

6.1 Classification – Authentication

In the field of classification, and more generally regarding pattern recognition, there are two main ways to create models which depend on whether information is available on the groups of objects to be classified: the so-called supervised and unsupervised pathways. To classify samples by geographical region, type, or variety, EEM fluorescence associated with chemometric tools is a real asset. For example, 3D fluorescence spectroscopy is a good solution for the classification of wines by grape variety and/or geographical area.[50,121]

However, a visual analysis of the spectra does not always enable their direct interpretation. On the one hand, it is difficult to make an overall comparison of all the spectra simultaneously without a computer tool, while on the other, the fluorescence matrices obtained are by construction a superimposition of the fluorescence of several fluorophores that might be present in the sample. It is, therefore, necessary to use a signal extraction method to reveal the different components in the recorded signal and thus better classify the wines in separate groups. It will also be possible to identify the corresponding fluorophores from the excitation–emission wavelength pairs present on the separate components of the signal. In this section, we present one example using PARAFAC as the signal extraction method[50,121] and another that implements ICA.[122]

A recent study of 57 wines (Figure 19) used the PARAFAC analysis with a four-component model, C1 to C4. In parallel, an HPLC analysis was performed to calibrate the PARAFAC components with the concentrations of some chemical compounds of interest in the wine samples, and particularly polyphenols. Deconvolution of the signal obtained using PARAFAC on the fluorescence data made it possible to demonstrate a certain specificity of the PARAFAC components thus calculated. For example, it can be seen that component C1 had a maximum excitation at about 260 nm and a maximum emission at 380 nm, so was not specific to a single family of compounds; it could be closer to either phenolic acids, t-resveratrol or anthocyanins.[50] The C2 component tended to correspond to catechin and epicatechin because its profile and emission and excitation maxima were close to those might be seen for the spectra of these compounds. The C3 component tended to correspond to p-coumaric acid, t-resveratrol, t-piceid acid, and gentisic acid, and C4 was associated with vanillic acid. Figure 20 shows the different factorial planes that tended to be associated with the 'regional' effect (Figure 20a) or with the 'grape variety' effect (Figure 20b). The plane formed by C1 and C4 made it possible to visualize the distribution of the different groups of wines within the multivariate space formed by these two PARAFAC components. The geographical origin effect is very clear, with the Australian and Spanish samples being distinctly different from the other samples on C1. On the other hand, C4 was able to separate Chilean wines from American and

Encyclopedia of Analytical Chemistry, Online © 2006–2018 John Wiley & Sons, Ltd.

This article was published in the *Encyclopedia of Analytical Chemistry* in 2018 by John Wiley & Sons, Ltd.
DOI: 10.1002/9780470027318.a9540

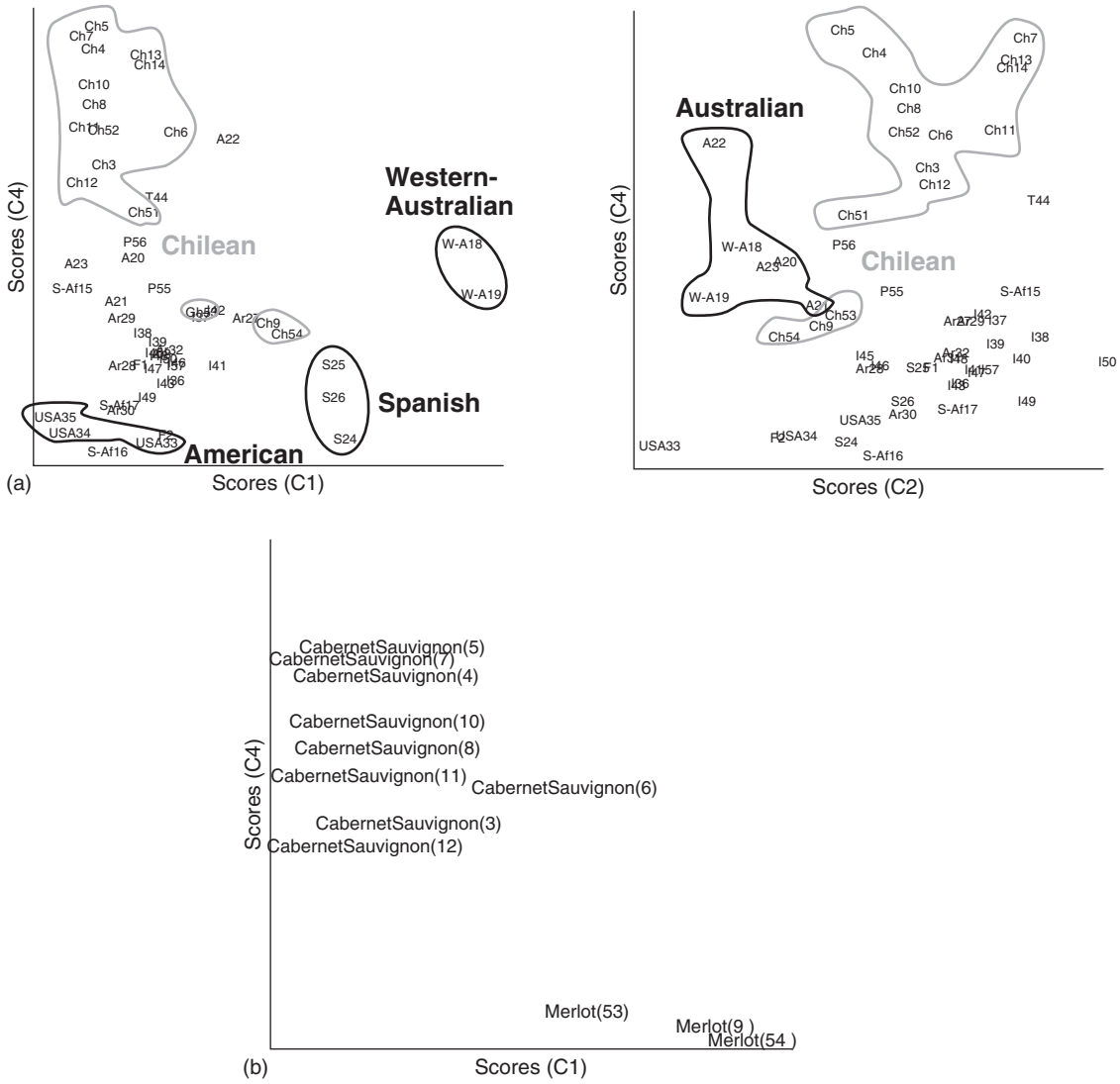

Figure 20 2D representations of PARAFAC scores corresponding to the fourth component against those corresponding to the first and second ones. Samples are represented according to the origin (a) and grape variety within Chilean samples (b) in A: F France, Ch. Chile S-Af South Africa S Spain Ar. Argentina A:Australia I:Italia P:Portugal.[50] (Reprinted with permission from Airado-Rodriguez, D., Duran-Meras, I., Galeano-Diaz, T., and Wold, J. P. (2011). Front-face fluorescence spectroscopy: A new tool for control in the wine industry. *Journal of Food Composition and Analysis* **24**, 257–264. Copyright 2011 American Chemical Society.)

Spanish wines because of a higher content in vanillic acid. The HPLC-FLD analysis produced results on three profiles: 262/364 nm, 275/320 nm, and 330/410 nm. Good correlations were observed between component 2 and catechin concentrations at 275/320 nm ($r^2 = 0.90$) and between component 1 and peaks at 260/360 nm on the chromatogram ($r^2 = 0.82$). A good correlation could also be observed between component 3 and the chromatogram at 330/410 nm. An alternative chemometric pathway was used to distinguish the grape varieties. Our research group proposed the use of ICA. To better highlight the differences between varieties from the chemistry of the samples, the fluorescence spectra were recorded at pH levels which differed from the natural pH[122] (Figure 21). Under the acid–base conditions selected, compounds that initially had little or no fluorescence became highly active due to an increase in electron density at the deprotonated base sites. Because electronic changes to the molecules have a significant impact on possible electronic delocalization, molecular fluorescence might be markedly impacted. This property was, therefore, exploited with respect to three grape varieties from three different sources. So, to observe the modification of the fluorescence, the pH of wines were modified to values 7 and 8, to compare with the natural pH which is around 3.5. The optimal ICA model thus calculated

Encyclopedia of Analytical Chemistry, Online © 2006–2018 John Wiley & Sons, Ltd.

This article was published in the *Encyclopedia of Analytical Chemistry* in 2018 by John Wiley & Sons, Ltd.
DOI: 10.1002/9780470027318.a9540

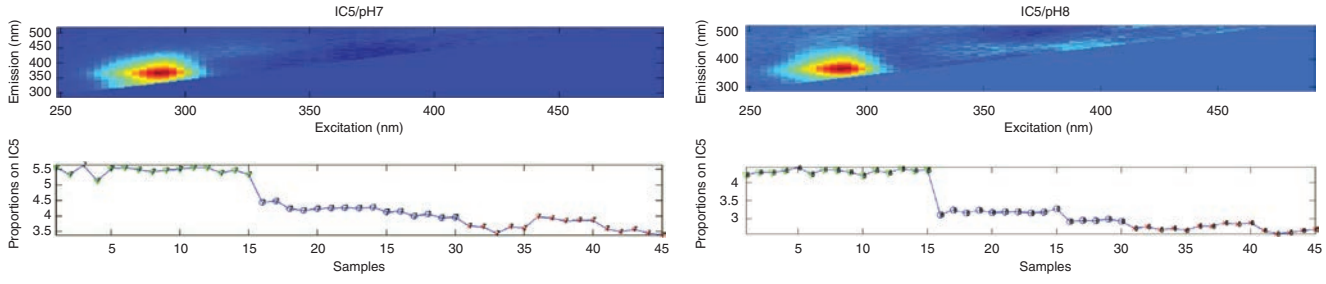

Figure 21 ICS proportions and signals – IC5/pH7 and IC5/pH8.

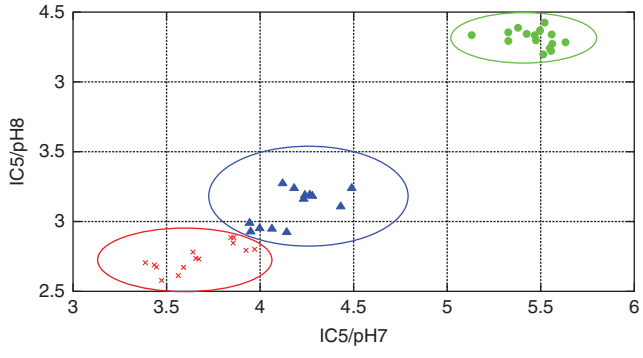

Figure 22 Proportions of IC5 at pH 8 vs IC5 at pH 7. Shiraz (x), Pinot noir (o), and Cabernet Sauvignon (Δ). (Reproduced with permission from Elsevier. © 2016.[122])

included seven ICs. The IC5 scores and signals at pH 7 and pH 8 could be represented (Figure 22). IC5 at pH7 and pH8 had a maximum of 280/380 nm fluorescence that approximated to the wavelengths of anthocyanins.[121,122] The scores of the two ICs were then represented on the factorial plane. There was good discrimination of grape varieties, especially Pinot Noir, as this contains more anthocyanins than the other two grape varieties studied.

In the field of paint materials, total SFS can be used with chemometric tools such as PCA or hierarchical cluster analysis (HCA) to classify organic paint materials such as protein-based binding media, drying oils, or varnish. The originality of this technology is that the spectra are standardized and used in the form of polar coordinate contours with a common origin. PCR is then performed on the polar coordinates of the contours and the scores of the first two PCA components are used as inputs for HCA. In this case, PCA is used to reduce the dimensions of the initial dataset. The dendrogram supplies information on the origin and chemical composition of the paint materials. Figure 23 shows four different groups: (i) shellac (the most distinctive); (ii) casein, egg, and isinglass (a more heterogeneous group); (iii) drying oils; and (iv) mastic and dammar (a more homogeneous group).

The aging and authenticity of vinegars have also been studied using 3D fluorescence associated with different chemometric methods such as PARAFAC, PLS-DA, and SVM.[123] Indeed, the idea is to link certain techniques in order to build a treatment process that will generate a classification model. First, a signal extraction method such as PARAFAC is used to characterize and discriminate the vinegars, and then a supervised method such as PLS-DA or SVM is applied to build a classification model. PLS-DA is a PLS2-based classification method[124] in which the groups are known in advance and the variable to be explained from a categorical standpoint is a matrix of the different classes called matrix indicators. The PLS components are calculated to rank the samples in the given groups within the columns of the indicator matrix. SVM is able to perform both linear and nonlinear classifications[125] and can reformulate the ranking as a quadratic optimization problem. The goal is to determine an optimal separation hyperplane (OSH) between the different classes so as to enable the classification of unknown samples. Maximizing the distance (or margin) between the hyperplane and the samples closest to the learning set can achieve this. PARAFAC enables the extraction of more or less specific loadings of each fluorophore (Figure 24), and their intensity is related to the fluorophore concentration in the sample. To model the separation between the groups, PLS-DA and SVM were applied on the PARAFAC loadings of the mode samples. Figure 24 shows the results with loadings on the excitation mode (top left), loadings on the emission mode (top right), and the factorial plane formed by the first two PARAFAC components on the sample mode. This study showed the superiority of SVM over PLS-DA in solving classification problems where groups are not clearly separated by a plane or hyperplane. In some cases, the chemical similarities of samples cannot be modeled using a linear factor model such as PARAFAC, which is no more than a generalization of the PCA, so that the discrimination between the groups remains poor. Otherwise the original example is the study of various Chinese traditional medicinal powders (called TCMs) using fluorescence spectroscopy and chemometrics.[126] Two medicinal herbs from the TCMs *Cortex Phellodendri Chinensis* (CPC) and *Cortex Phellodendri Amurensis*

Encyclopedia of Analytical Chemistry, Online © 2006–2018 John Wiley & Sons, Ltd.

This article was published in the *Encyclopedia of Analytical Chemistry* in 2018 by John Wiley & Sons, Ltd.
DOI: 10.1002/9780470027318.a9540

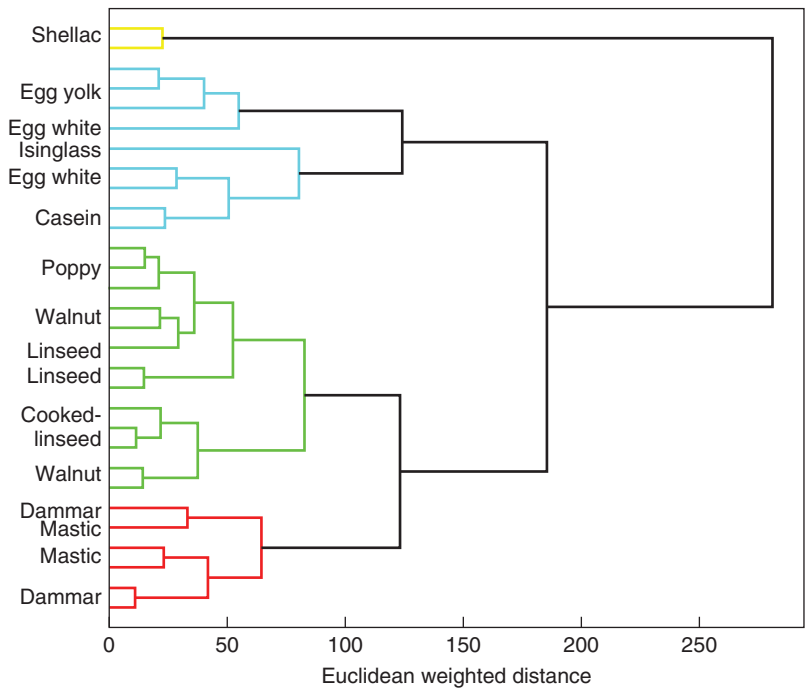

Figure 23 Dendrogram representation of results of hierarchical cluster analysis of polar graphs of fluorescence spectra of 11 different media (excluding copal) following filtering of data. Clusters of four different colors are formed beneath a threshold distance of 100 based on the weighted Euclidean distance between spectra. (Reprinted with permission from Nevin, A., Comelli, D., Valentini, G., and Cubeddu, R. (2009). Total Synchronous Fluorescence Spectroscopy Combined with Multivariate Analysis: Method for the Classification of Selected Resins, Oils, and Protein-Based Media Used in Paintings. Analytical Chemistry 81, 1784–1791. Copyright 2009 American Chemical Society.[107])

(CPA) and two toxic samples *Caulis Mahoniae* (CM) and *David Poplar Bark* (DPB) were analyzed. Only DPB had a very different spectrum, the others being very similar. PROMETHEE and GAIA, two multi-criteria methods for decision support, have also been proposed in this context. Preference Ranking Organization METHod for Enrichment Evaluation (PROMETHEE) is an ordered classification method; it produces quantitative indices φ, reflecting a relative performance of objects within a group. The objective is to rank the decisions from best to least good and to implement compromises. The chosen function is Gaussian. The PC scores are used as variables to which a reference object is assigned. High value (positive) scores are preferentially determined by φ, the net value of the classification index. The closest φ values are associated with the most similar objects and inversely, with the most different φ values are associated the most different objects. Thus the range of values of the φ index ranges from the most positive to the most negative. GAIA (geometrical analysis for iterative assistance) highlights conflicting any criteria, identifies trade-offs and helps to set priorities. GAIA produces a two-dimensional graph (Figure 25) from the PCA scores that reflects less than 100% of variance and is obtained using a matrix derived from the Promethean φ indices. In the spectra of samples containing a single ingredient, it is excitation wavelengths with a higher φ index that best discriminate samples in terms of their emission wavelengths. This method produces interesting values but unfortunately does not discriminate the entire dataset, i.e. medicinal plants that are tested alone or mixed.

6.2 Quality Assessment – Quality Control

Evaluating quality does not necessarily target the same aspects, depending on whether the study concerns food, animals, or humans. For food products, quality includes several components such as nutritional health and organoleptic quality. Therefore, in order to improve nutritional quality, it is interesting to characterize a food in order to determine its content in sugars or trans-fatty acids, to control oxidation and gain a clearer understanding of elements that are positive for health such as polyphenols. A health quality assessment integrates a risk assessment of contamination and, as mentioned in Section 5.2, fluorescence offers a means to detect fluorescent contaminants with some success. As for organoleptic quality, this can be determined using sensory analysis

Encyclopedia of Analytical Chemistry, Online © 2006–2018 John Wiley & Sons, Ltd.

This article was published in the *Encyclopedia of Analytical Chemistry* in 2018 by John Wiley & Sons, Ltd.
DOI: 10.1002/9780470027318.a9540

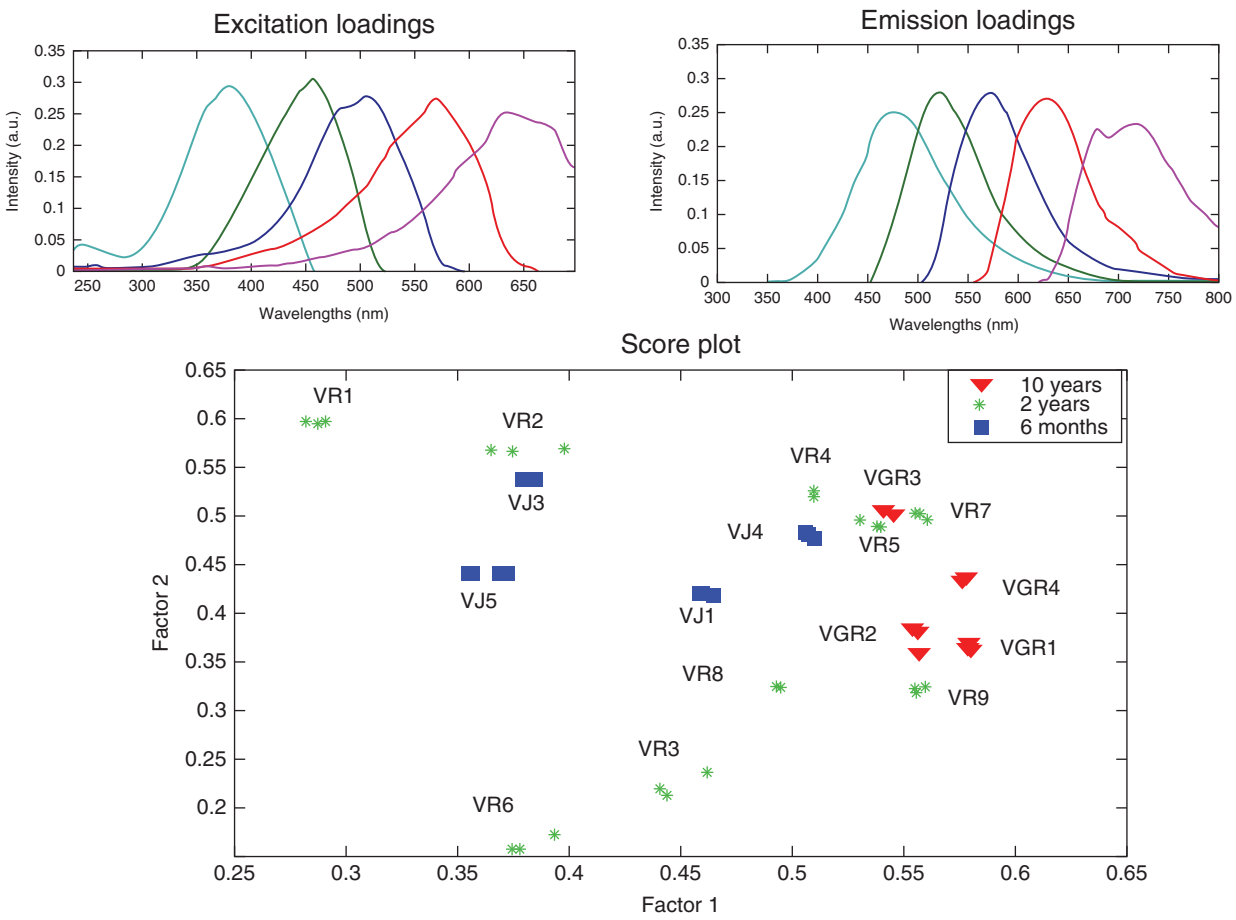

Figure 24 PARAFAC results obtained by using EEMizer. Best model with five factors. The scores plot depict the relationship between Factors 1 and 2 (blue and green, respectively, in the excitation–emission loadings). (Reproduced with permission from Elsevier. © 2012.[123])

and studies of food behavior which can help to reveal consumer preferences.

A more objective approach to the evaluation of food quality is physicochemical analysis which is increasingly being supplemented by spectroscopic methods which can contribute simplicity and sensitivity and have the advantage of being noninvasive, so in most cases, they are very rapid. It is in this context that fluorescence spectroscopy has been used to evaluate the quality or freshness of fish, the oxidation state of olive oil or the quality of milk. In the same way as supervised classification, it is necessary to evaluate the quality of a food in order to obtain a quantitative indicator or scale of measurement for this quality, in addition to fluorescence spectra. Once again, the use of chemometrics to link spectral data with quantitative or qualitative data has become standard. Thus, in the field of quality, the most widely used methods are PLS or DA. To estimate the freshness of frozen intact fish (in Japan), 3D fluorescence spectroscopy was used and the findings compared with the freshness index.[127,128] The idea was to develop a rapid and noninvasive method to avoid thawing the fish samples that could distinguish fresh fish from those whose state of conservation was less good and seeing the appearance of biogenic amines such as histamine, putrescine, cadaverine, etc. Thus EEM spectral acquisition was performed on intact frozen fish using an optical fiber. The concentration of ATP and its degradation products (e.g. ADP, AMP, IMP) was analyzed using HPLC-UV in order to determine the *K*-value of the freshness index, which was calculated as the ratio between the metabolites of nonphosphorylated ATP and all the degradation products of ATP.

$$K\text{-value}(\%) = \frac{\text{HxR} + \text{Hx}}{\text{ATP}+\text{ADP}+\text{AMP}+\text{IMP}+\text{HxR}+\text{Hx}} \times 100$$

ATP, adenosine tri-phosphate; ADP, adenosine di-phosphate; AMP, adenosine mono-phosphate; IMP,

Encyclopedia of Analytical Chemistry, Online © 2006–2018 John Wiley & Sons, Ltd.

This article was published in the *Encyclopedia of Analytical Chemistry* in 2018 by John Wiley & Sons, Ltd.
DOI: 10.1002/9780470027318.a9540

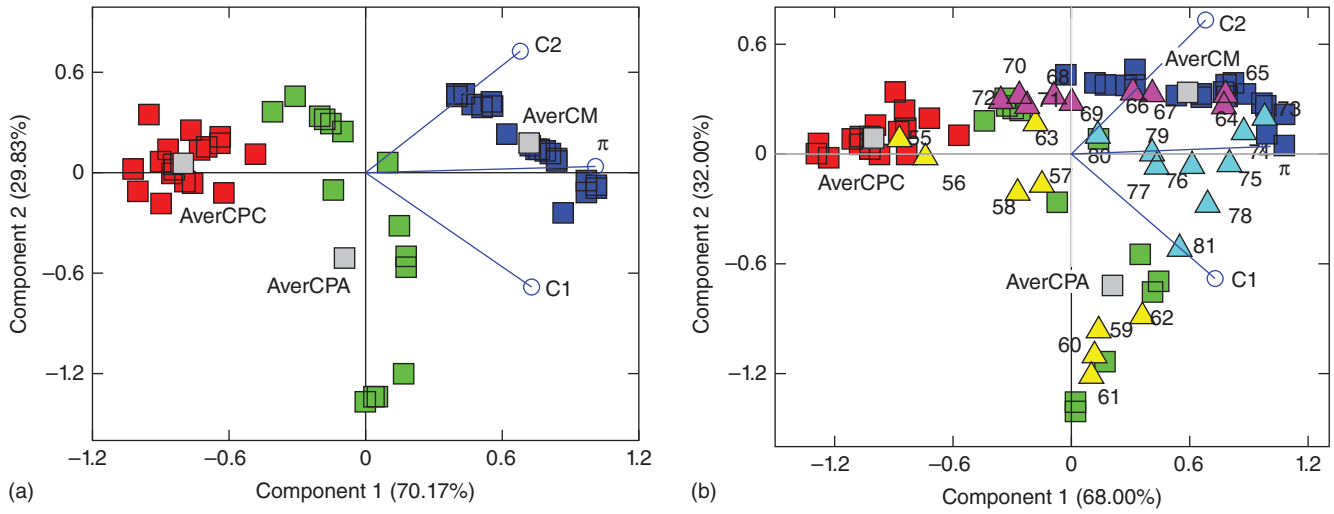

Figure 25 GAIA biplot of all the samples involved: excitation data for CPC, CPA, CM (a), and those with their mixtures (b); scores of the first three PCs from the scaled data were used as input variables; the GAIA display component 1 versus component 2 biplot explaining 100% of the input data variance. (Reprinted with permission from Gu, Y., Ni, Y., and Kokot, S. (2012). Solid Phase Excitation-Emission Fluorescence Method for the Classification of Complex Substances: Cortex Phellodendri and Other Traditional Chinese Medicines as Examples. The Journal of Physical Chemistry A 116, 8949–8958. Copyright 2012 American Chemical Society.[126])

inosine-5′-monophosphate; HxR, inosine; Hx, hypoxanthine.

Three classes of samples were considered in this problem: 'first freshness', 'fresh', 'not fresh'. A PLS regression of the Freshness index performed on the unfolded fluorescence data made it possible to evaluate the freshness of the frozen fish. Another specific algorithm was also developed in order to select a combination of excitation and emission wavelengths within the set of EEM spectra that was specific to detecting changes to the freshness of frozen fish (Figure 26). The authors demonstrated a reasonable prediction of freshness indices ($r^2 = 0.89$) and an acceptable classification rate (87.5%) of the fish samples. The problem with this type of study is to obtain sufficient samples per class whose quality needs to be predicted. Models often fail because of a lack of robustness, and statistical representativeness is often limited to local production and does not cover all production in a region or country.

Known for its health benefits, olive oil needs to be analyzed in terms of both its authenticity and its geographical origin. Thus in the study by Guzman et al.,[129] the objective was to determine whether the fluorescence-PLS combination enabled the efficient evaluation of quality indices: peroxide index, K232, K270, and acidity. Peroxide is an indicator of primary oxidation products and K232 and K270 of secondary oxidation products, and they correspond to fluorescence emission between 450 and 600 nm. There was a good correlation between Guzman's and Guimet's results[67] indicating that fluorescence can 'capture' enough information to enable a correct estimation of peroxide indices ($r^2 = 0.84$) and K270 ($r^2 = 0.9$).

For the health assessments, the development of a predictive 3D fluorescence spectroscopy method to determine aerobic cells on the surface of beef may prove to be a useful tool to control the risk of poisoning. The study by Yoshimura et al.[54] focused on this issue with respect to different storage periods. Microbiological counts (APC, aerobic plate count) and fluorescence spectroscopy analysis were performed in parallel. Several endogenous fluorophores were detected and their evolution followed over time: tryptophan, NADH, porphyrin, and flavin. Tryptophan may arise from protein residues, bacteria, or meat. Its level falls as the germ content rises, suggesting a loss of amino acids in the meat due to their consumption by bacteria. For other fluorophores, combining the results of previous studies with an observed trend showed that, for example the fluorescence of NAD(P)H increased when bacteria such as *Pseudomonas* were growing. Overall, PLS model predictions performed on the fluorescence spectra revealed a good correlation, despite the variability of autofluorescence intensities related to bacterial flora and to the state of muscles and adipose tissues in the beef.

Evaluating the quality of samples using fluorescence spectroscopy is thus able to discriminate samples versus a quality criterion for health purposes[54,127,129] or for authentication.[129]

Encyclopedia of Analytical Chemistry, Online © 2006–2018 John Wiley & Sons, Ltd.

This article was published in the *Encyclopedia of Analytical Chemistry* in 2018 by John Wiley & Sons, Ltd.
DOI: 10.1002/9780470027318.a9540

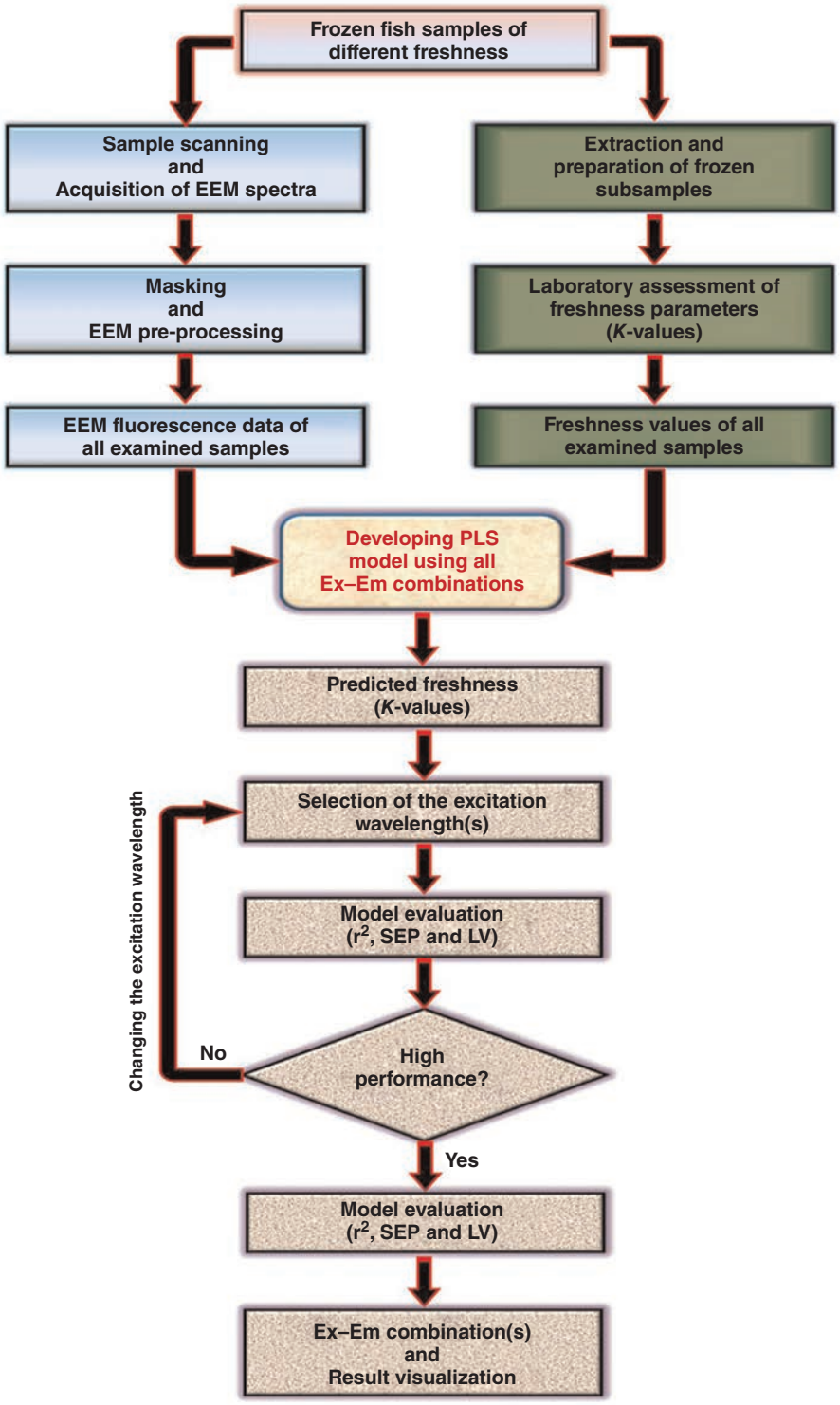

Figure 26 Flow chartshowing all steps involved in predicting freshness of frozen fish samples. (Reproduced with permission from Elsevier. © 2015.[127])

Encyclopedia of Analytical Chemistry, Online © 2006–2018 John Wiley & Sons, Ltd.

This article was published in the *Encyclopedia of Analytical Chemistry* in 2018 by John Wiley & Sons, Ltd.
DOI: 10.1002/9780470027318.a9540

6.3 Process Indicators: Thermal and Photonic

3D fluorescence spectroscopy is a good indicator of changes to spectral fingerprints during processes such as heating. The case of vegetable oils is a good example. Indeed, during heating, and particularly frying, vegetable oils undergo complex chemical thermo-oxidation, polymerization, cis/trans isomerization, and cyclisation reactions. This affects the nutritional and organoleptic characteristics of the oil and results in the formation of compounds that can be harmful to health such as trans isomers and malondialdehyde, which is potentially toxic because it reacts easily to form DNA adducts, and especially M1G (pyrimido[1,2-α] purine-10(3H)–one), which is mutagenic.

Numerous articles have reported the value of 3D fluorescence spectroscopy to observing the temperature-related course of degradation of vegetable oils. Reference can be made to the kinetic study on the heating of Tunisian vegetable oils at different temperatures, with or without the addition of an antioxidant.[69] The application of ICA to the unfolded fluorescence cube made it possible to extract the fluorescence signals related to antioxidants such as vitamin E, which declines less rapidly when a natural secondary antioxidant such as an organic extract of Nigel is added. Another study on olive oil revealed the usefulness of 3D fluorescence analysis followed by PARAFAC when monitoring heating-related changes affecting fluorophores, which are notably observed with respect to oxidation products (tocopherols) and could be linked to standard analyses of polar compounds, tocopherols, etc., performed elsewhere on the samples.[70,130]

With respect to cookie manufacturing, synchronous frontal fluorescence has been used to rapidly estimate levels of neoformed contaminants generated during the manufacturing process.[13] Various compounds such as carboxymethyllysine (CML) and hydroxymethylfurfural (HMF), as well as acrylamide, were analyzed conventionally using GC-MS-MS and HPLC. Different types of dough and cooking methods were studied. Synchronous fluorescence two-dimensional spectra were recorded and transformed into excitation–emission matrices (Figure 27). The PARAFAC breakdown produced five fluorescence profiles containing tryptophan (Trp), riboflavin (Rf), and three newly formed compounds (Nf1, Nf2, Nf3) (Figure 28). For example, cookies made using glucose might have lower tryptophan fluorescence and more intense riboflavin profiles than those made with sucrose. A high-saturated fatty acid content favored lower levels of neoformed compounds (Nf1) and higher concentrations of riboflavin (Rf) versus cookies made

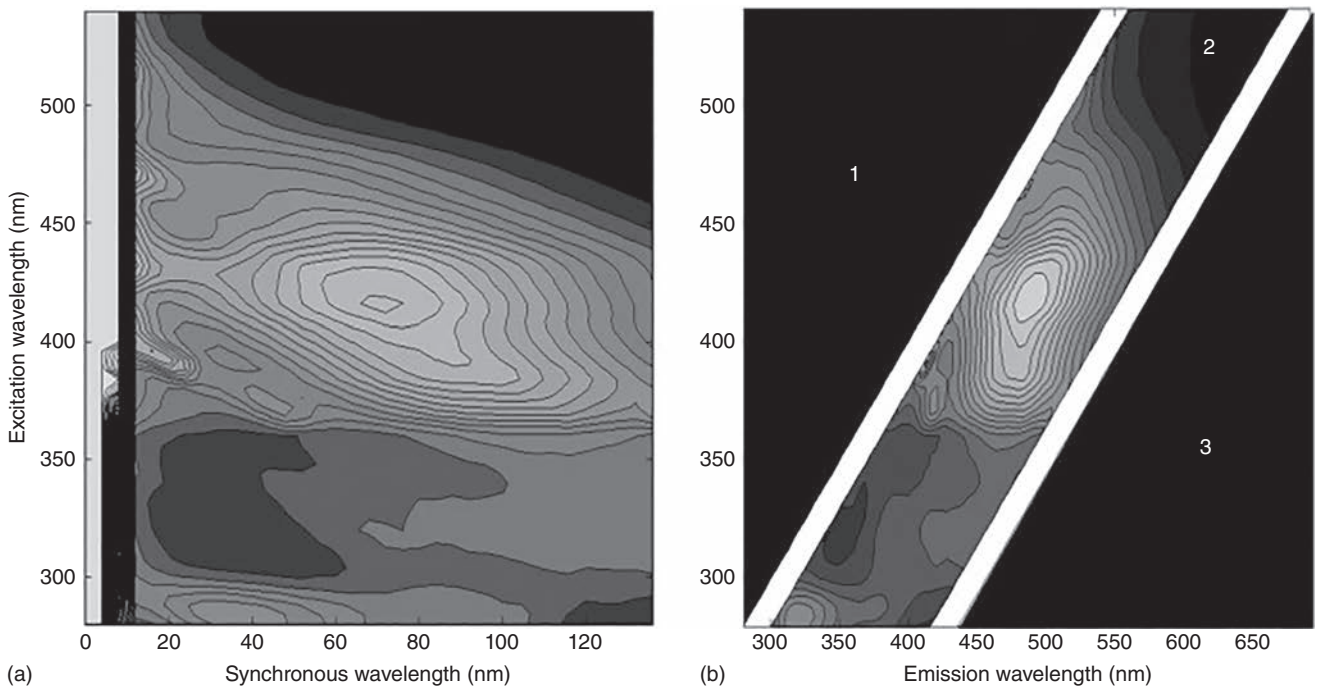

Figure 27 Two dimensional synchronous spectra (a) shifted to EEM (b) positions. In (b) the two ribbons of missing values (white bands) were used to replace the first order Rayleigh scatter and regions adjacent to the fluorescence signal acquired at the maximum synchronous delta. Regions 1 and 3 missing values created upon shifting the two dimensional EEM were replaced by zeros. (Reproduced with permission from Elsevier. © 2008.[13])

Encyclopedia of Analytical Chemistry, Online © 2006–2018 John Wiley & Sons, Ltd.

This article was published in the *Encyclopedia of Analytical Chemistry* in 2018 by John Wiley & Sons, Ltd.
DOI: 10.1002/9780470027318.a9540

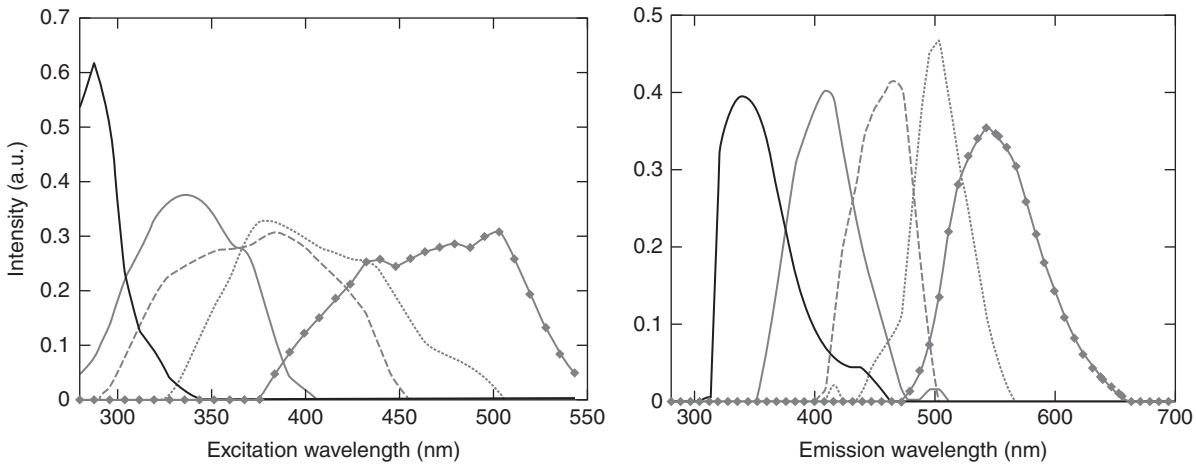

Figure 28 PARAFAC spectral loadings from three-way arrangement of experimental kinetic data EEMs. (Reproduced with permission from Elsevier. © 2008.[13])

with a low saturated fat content. The study reported that a regression model for the acrylamide, CML, and HMF concentrations on PARAFAC loadings of the sample mode indicated that the intensities of the fluorescence profiles clearly discriminated the critical steps in the baking process and facilitated the prediction of Acrylamide, CML, and HMF neoformed compounds in the cookies.[13]

In another area, 3D fluorescence combined with a multiway technique such as PARAFAC, MCR, and N-PLS can be used to analyze the degradation of a cell culture medium caused by exposure to ambient light in the visible range.[131] Photodegradation resulted in spectral changes and the breakdown of PARAFAC and MCR findings revealed five factors: Trp, Tyr, pyridoxine (Py), folic acid (FA), and (Rf). Using this fast method, it was possible to determine and quantify the course of photodegradation. These different examples, therefore, show that fluorescence spectroscopy analysis combined with appropriate chemometrics tools can be effective in determining the criteria to monitor and control thermal[13,69] or photonic industrial processes.[131]

6.4 Adulteration

Adulteration constitutes economic fraud. In order to reduce production costs, fraudulent adulteration practices add value to the by-products of industry or enable the use of low-cost, imported raw materials. All food sectors are subject to market regulation and have to deal with the issue of adulteration. Adulteration can also cause a loss of nutritional or functional properties. It would be difficult to list all products that are commonly adulterated, but because the objective is economic gain, those most likely to be affected are foods with high added value. They may be commercially for various reasons, notably if they are essential foodstuffs such as meat or milk where there is a need to produce greater quantities and more cheaply. Products that can be categorized as 'luxury' or 'local' products may also be of interesting with respect to adulteration[132] especially if they are exported because their production is regional, such as specific types of olive oil, honey, fruit puree, etc., and the amounts produced are not as large as for staples. A third category of high added value food products should also be taken into account, which are those that are not essential to our diet but whose tonnages are considerable, such as coffee or wine. These products occupy an essential role in our cultures and societies, as is the case, for example in Mediterranean populations. A report from the European Parliament[132] presented a list of the principal foods most subject to fraud: olive oil, fish, organic foods, milk, cereals, and honey. A collateral effect of food fraud is an increase in health risks. Indeed, the manipulations involved in producing counterfeits introduce both a chemical/microbiological risk and allergic risk, the consequences of which may be important to the health of consumers. The need for technical advances in fraud detection has led researchers to continually test new technologies. 3D fluorescence is one of the techniques whose applications have developed considerably during the past 15 years in terms of detection fraudulent foods. A dual approach needs to be adopted, because in some cases it may be easier to detect the adulterant by following a so-called 'targeted' analytical approach, whereas in others it will be more effective to use a global analytical approach to obtain 'footprints'. If we consider the case of honey, both approaches may be useful, depending on the type of sugar syrup that has been added. If the

Encyclopedia of Analytical Chemistry, Online © 2006–2018 John Wiley & Sons, Ltd.

This article was published in the *Encyclopedia of Analytical Chemistry* in 2018 by John Wiley & Sons, Ltd.
DOI: 10.1002/9780470027318.a9540

latter is derived from sugar cane, targeted research on the presence of sclereous rings or parenchymal cells directly from the plant will be sufficient. On the other hand, if the syrup was made by the hydrolysis of wheat or corn starches, no cell tracer can be detected and a more global 'fingerprint' approach may be more efficient,[133] using stable carbon isotopic measurements of the entire sample and the protein fraction (internal standard stable carbon isotope ratio method (ISCIRA)).[134–136] 3D-fluorescence can be applied under a global footprint approach. For example, this was the case of a study which focused on the addition of rice syrup to different types of honey.[137] Modelling of this adulteration was performed using both PLS regression and a multilayer neural network (artificial neural network, ANN). It can be seen that these methods are evolving toward more complex artificial intelligence techniques that are also more able to take account of a greater complexity in the information to be processed. Back propagation artificial neural network (BP-ANN) type neural networks are the most common and can, through a learning process, classify honey samples as either 'authentic' or 'adulterated', or regress the weights of the layer of output on a vector containing the percentage adulteration of the samples. As with a PLS regression, it is then possible to estimate the adulteration rate of the samples for a given adulterant and within a given range of adulteration.[137]

A fraud detection approach that uses both fluorescence spectral fingerprinting and the determination of another physicochemical quantity by a reference method has now become conventional and demonstrated its effectiveness with respect to numerous food products: honey,[137] orange juice,[138] brandy,[139] olive oil,[16] milk,[63] etc.

7 CONCLUSION

3D or frontal fluorescence is a technique that has applications in many areas. The chemometric tools most commonly associated with it enable a clearer understanding of the data generated. These tools can be used alone or in combination in order to enhance the extraction of useful information or maximize performance in a variable classification or in a predictive regression process.

Fluorescence data offer a spectral fingerprint which enables the characterization of samples in a very important space of variability, such as that which is inherent in food samples. Thus fluorescence spectroscopy will find a broad range of applications that will ensure its equal efficiency in foods and in biological substances such as urine, feces, animal tissues, or environmental samples. Most of these applications are still qualitative, although quantitative methods are available. It will readily be understood that the use of 3D fluorescence fingerprinting is more suitable for recognition, classification or detection processes where rapidity and sensitivity are crucial.

ACKNOWLEDGMENTS

We would to thank the Professor Douglas N. Rutledge for his support and help about the writing of the manuscript.

ABBREVIATIONS AND ACRONYMS

ANN	Artificial Neural Network
APC	Aerobic Plate Count
ATR	Attenuated Total Reflection
BI	Business Intelligent
BP-ANN	Back Propagation Artificial Neural Network
BSA	Bovine Serum Albumin
CCD	Charge Coupled Device
DFA	Discriminant Factor Analysis
DOM	Dissolved Organic Matter
EEM	Excitation Emission Matrix
FRI	Fluorescence Regional Integration
GAIA	Geometrical Analysis for Iterative Assistance
GFP	Green Fluorescent Protein
HCA	Hierarchical Cluster Analysis
IC	Independent Component
ICA	Independent Component Analysis
ISCIRA	Internal Standard Stable Carbon Isotope Ratio Method
MCR-ALS	Multivariate Curve Resolution-alternating Least Square
NAD	Nicotinamide Adenine Dinucleotide
NADPH	Nicotinamide Adenine Dinucleotide Phosphate (forme réduite)
OSH	Optimal Separation Hyperplane
PAH	Polycyclic Aromatic Hydrocarbon
PARAFAC	Parallel Factors Analysis
PCA	Principal Component Analysis
PLS-DA	Partial Least Squares-Discriminant Analysis
PLS	Partial Least Squares
PROMETHEE	Preference Ranking Organization METHod for Enrichment Evaluation
SFS	Synchronous Fluorescence Spectroscopy
SVM	Support Vector Machine
TCM	Traditional Medicinal Powder
U-PLS/RBL	Unfolded Partial Least Squares Coupled to Residual Bilinearization

Encyclopedia of Analytical Chemistry, Online © 2006–2018 John Wiley & Sons, Ltd.

This article was published in the *Encyclopedia of Analytical Chemistry* in 2018 by John Wiley & Sons, Ltd.
DOI: 10.1002/9780470027318.a9540

RELATED ARTICLES

Electronic Absorption and Luminescence
Ultraviolet and Visible Molecular Absorption and Fluorescence Data Analysis • Investigation of Pollution in Rivers and Groundwater by Fluorescence

Environment: Water and Waste
Luminescence in Environmental Analysis

Environmental Analysis and Related Instrumentation
The Use of 3D Fluorescence and Its Decomposition in Environmental Organic Matter Studies

Food
Fluorescence Spectroscopy in Food Analysis

Peptides and Proteins
Fluorescence Spectroscopy in Peptide and Protein Analysis

REFERENCES

1. B. Valeur, *Invitation à la fluorescence moléculaire*, De Boeck, Bruxelles, 2004.
2. B. Valeur, *Lumière et luminescence, Ces phénomènes lumineux qui nous entourent*, Belin, Paris, 2017.
3. S. Martrenchard-Barra, 'Luminescence', Universalis éducation [en ligne]. Encyclopædia Universalis, consulted on 16 June 2017, 2017.
4. D.W. Johnson, J.B. Callis, G.D. Christian, 'Rapid Scanning Fluorescence Spectroscopy', *Anal. Chem.*, **49**, 747A–757A (1977).
5. T.J. Porro, D.A. Terhaar, 'Double-Beam Fluorescence Spectrophotometry', *Anal. Chem.*, **48**, 11103A–11107A (1976).
6. T. Thilivhali, I.M. Warner, 'Applications of Multidimensional Absorption and Luminescence: Spectroscopies in Analytical Chemistry', *Chem. Rev.*, **91**, 493–507 (1991).
7. Y. Senga, S. Minami, 'Excitation-Emission Matrix Scanning Spectrofluorometer', *Appl. Spectrosc.*, **45**, 1721–1725 (1991).
8. J.R. Lakowicz, *Principles of Fluorescence Spectroscopy*, 3rd edition, Springer, New York, 2006.
9. J.-R. Albani, *Absorption et Fluorescence: principes et applications*, Editions Tec-Doc, Paris, 2001.
10. G.G. Guibault, *Practical Fluorescence*, M. Dekker, New York, 1991.
11. D. Patra, A.K. Mishra, 'Recent Developments in Multi-Component Synchronous Fluorescence Scan Analysis', *TrAC Trends Anal. Chem.*, **21**, 787–798 (2002).
12. E. Sikorska, I. Khmelinskii, M. Sikorski, 'Analysis of Olive Oils by Fluorescence Spectroscopy: Methods and Applications', in *Olive Oil - Constituents, Quality, Health Properties and Bioconversions*, ed D.D. Boskou, Intech Europe, Rijeka, 2012.
13. J. Rizkallah, F.J. Morales, L. Ait-ameur, V. Fogliano, A. Hervieu, M. Courel, I. Birlouez Aragon, 'Front Face Fluorescence Spectroscopy and Multiway Analysis for Process Control and NFC Prediction in Industrially Processed Cookies', *Chemom. Intell. Lab. Syst.*, **93**, 99–107 (2008).
14. K. Kumar, A.K. Mishra, 'Analysis of Dilute Aqueous Multifluorophoric Mixtures Using Excitation-Emission Matrix Fluorescence (EEMF) and Total Synchronous Fluorescence (TSF) Spectroscopy: A Comparative Evaluation', *Talanta*, **117**, 209–220 (2013).
15. J. Christensen, L. Norgaard, R. Bro, S.B. Engelsen, 'Multivariate Autofluorescence of Intact Food Systems', *Chem. Rev.*, **106**, 1979–1994 (2006).
16. K.I. Poulli, G.A. Mousdis, C.A. Georgiou, 'Rapid Synchronous Fluorescence Method for Virgin Olive oil Adulteration Assessment', *Food Chem.*, **105**, 369–375 (2007).
17. K. Abbas, R. Karoui, A. Aït-Kaddour, 'Application of Synchronous Xuorescence Spectroscopy for the Determination of Some Chemical Parameters in PDO French Blue Cheeses', *Eur. Food Res. Technol.*, **234**, 457–465 (2012).
18. J. Eisinger, J. Flores, 'Front-Face Fluorometry of Liquid Samples', *Anal. Biochem.*, **94**, 15–21 (1979).
19. J. Sadecka, J. Tothova, 'Fluorescence Spectroscopy and Chemometrics in the Food Classification – a Review', *Czech J. Food Sci.*, **25**, 159–173 (2007).
20. D.I.C. Kells, J.D.J. O'Neil, T. Hofmann, 'A Method for Eliminating Rayleigh Scattering from Fluorescence Spectra', *Anal. Biochem.*, **139**, 316–318 (1984).
21. D. Jouan-Rimbaud Bouveresse, H. Benabid, D.N. Rutledge, 'Independent Component Analysis as a Pretreatment Method for Parallel Factor Analysis to Eliminate Artefacts from Multiway Data', *Anal. Chim. Acta*, **589**, 216–224 (2007).
22. R.D. JiJi, K.S. Booksh, 'Mitigation of Rayleigh and Raman Spectral Interferences in Multiway Calibration of Excitation Emission Matrix Fluorescence Spectra', *Anal. Chem.*, **72**, 718–725 (2000).
23. P.H.C. Eilers, P.M. Kroonenberg, 'Modeling and Correction of Raman and Rayleigh Scatter in Fluorescence Landscapes', *Chemom. Intell. Lab. Syst.*, **130**, 1–5 (2014).
24. J. Workman, 'The State of Multivariate Thinking for Scientists in Industry: 1980–2000', *Chemom. Intell. Lab. Syst.*, **60**, 13–23 (2002).
25. L.G. Thygesen, Ã. Rinnan, S. Barsberg, J.K.S. Moller, 'Stabilizing the PARAFAC Decomposition of Fluorescence Spectra by Insertion of Zeros Outside the Data Area', *Chemom. Intell. Lab. Syst.*, **71**, 97–106 (2004).

Encyclopedia of Analytical Chemistry, Online © 2006–2018 John Wiley & Sons, Ltd.

This article was published in the *Encyclopedia of Analytical Chemistry* in 2018 by John Wiley & Sons, Ltd.
DOI: 10.1002/9780470027318.a9540

26. S. Wold, K. Esbensen, P. Geladi, 'Principal Component Analysis', *Chemometr. Intell. Lab. Syst.*, **2**, 37–52 (1987).
27. H. Hotelling, 'Analysis of a Complex of Statistical Variables into Principal Components', *J. Educ. Psychol.*, **24**, 417–441 (1933).
28. J.F. Cardoso, 'High-Order Contrasts for Independent Component Analysis', *Neural Comput.*, **11**, 157–192 (1999).
29. J.V. Stone, 'Independant Component Analysis: An Introduction', *Trends Cogn. Sci.*, **6**, 59–64 (2002).
30. D.N. Rutledge, D. Jouan-Rimbaud Bouveresse, 'Independent Components Analysis with the JADE Algorithm', *TrAC Trends Anal. Chem.*, **50**, 22–32 (2013).
31. D.N. Rutledge, D. Jouan-Rimbaud Bouveresse, 'Corrigendum to "Independent Components Analysis with the JADE Algorithm"', *TrAC Trends Anal. Chem.*, **67**, 220 (2015).
32. P. Valderrama, P.H. Março, N. Locquet, F. Ammari, D.N. Rutledge, 'A Procedure to Facilitate the Choice of the Number of Factors in Multi-way Data Analysis Applied to the Natural Samples: Application to Monitoring the Thermal Degradation of Oils Using Front-Face Fluorescence Spectroscopy', *Chemom. Intell. Lab. Syst.*, **106**, 166–172 (2010).
33. D. Jouan-Rimbaud Bouveresse, D.N. Rutledge, 'Independent Components Analysis: Theory and Applications', in *Resolving Spectral Mixtures, with Application from Ultrafast Spectroscopy to Super-Resoltion Imaging, Data Handling in Science and Technology*, Elsevier, Amsterdam, 2016.
34. R. Tauler, 'Multivariate Curve Resolution Applied to Second Order Data', *Chemom. Intell. Lab. Syst.*, **30**, 133–146 (1995).
35. R. Tauler, A. Smilde, B. Kowalski, 'Selectivity, Local Rank, Three-way Data Analysis and Ambiguity in Multivariate Curve Resolution', *J. Chemometr.*, **9**, 31–58 (1995).
36. J. Jaumot, A. de Juan, R. Tauler, 'MCR-ALS GUI 2.0: New Features and Applications', *Chemom. Intell. Lab. Syst.*, **140**, 1–12 (2015).
37. J.D. Carroll, J.J. Chang, 'Analysis of Individual Differences in Multidimensional Scaling Via an N-Way Generalization of Eckart-Young Decomposition', *Psychometrika*, **35**, 283–319 (1970).
38. R.A. Harshman, 'Foundations of the PARAFAC Procedure: Models and Conditions for an Explanatory Multimodal Factor Analysis', UCLA Working Papers in Phonetics, University Microfilms, Ann Arbor, MI, 16, 1–84, 1970.
39. R. Bro, H.A.L. Kiers, 'A new Efficient Method for Determining the Number of Components in PARAFAC Models', *J. Chemometr.*, **17**, 274–286 (2003).
40. F. Hitchcock, 'The Expression of a Tensor or a Polyadic as a sum of Products', *J. Math. Phys.*, **6**, 164–489 (1927).
41. C.M. Andersen, R. Bro, 'Practical Aspects of PARAFAC Modeling of Fluorescence Excitation-Emission Data', *J. Chemometr.*, **17**, 200–215 (2003).
42. R. Bro, 'PARAFAC. Tutorial and Applications', *Chemom. Intell. Lab. Syst.*, **38**, 149–171 (1997).
43. R. Bro, M. Vidal, 'EEMizer: Automated Modeling of Fluorescence EEM Data', *Chemom. Intell. Lab. Syst.*, **106**, 86–92 (2011).
44. S. Engelen, S. Frosch, B.M. Jørgensen, 'A Fully Robust PARAFAC Method for Analyzing Fluorescence Data', *J. Chemometr.*, **23**, 124–131 (2009).
45. S. Elcoroaristizabal, R. Bro, J.A. Garcia, L. Alonso, 'PARAFAC Models of Fluorescence Data with Scattering: A Comparative Study', *Chemom. Intell. Lab. Syst.*, **142**, 124–130 (2015).
46. C.B.Y. Cordella, 'PCA: The Basic Building Block of Chemometrics', in *Analytical Chemistry*, ed D.I.S. Krull, Intech Europe, Rijeka, 2012.
47. P. Geladi, B.R. Kowalski, 'Partial Least-Squares Regression: A Tutorial', *Anal. Chim. Acta*, **185**, 1–17 (1986).
48. C.M. Andersen, J.P. Wold, S.B. Engelsen, 'Autofluorescence Spectroscopy in Food Analysis', in *Handbook of Food Analysis Instruments*, ed S. Ötles, CRC Press, Boca Raton, FL, 347–363, 2008.
49. J. Christensen, Foodfluor- Food fluorescence library. Quality &Technology, Department of Food Science, Faculty of Science, University of Copenhagen, Denmark, http://www.models.life.ku.dk, 2005.
50. D. Airado-Rodriguez, I. Duran-Meras, T. Galeano-Diaz, J.P. Wold, 'Front-Face Fluorescence Spectroscopy: A new Tool for Control in the Wine Industry', *J. Food Compos. Anal.*, **24**, 257–264 (2011).
51. J. Mazina, M. Vaher, M. Kuhtinskaja, L. Poryvkina, M. Kaljurand, 'Fluorescence, Electrophoretic and Chromatographic Fingerprints of Herbal Medicines and Their Comparative Chemometric Analysis', *Talanta*, **139**, 233–246 (2015).
52. L. Poryvkina, N. Tsvetkova, I. Sobolev, 'Evaluation of Apple Juice Quality Using Spectral Fluorescence Signatures', *Food Chem.*, **152**, 573–577 (2014).
53. K. Wlodarska, K. Pawlak-Lemanska, I. Khmelinskii, E. Sikorska, 'Screening of Antioxidant Properties of the Apple Juice Using the Front-Face Synchronous Fluorescence and Chemometrics', *Food Anal. Methods*, **10**, 1582–1591 (2017).
54. M. Yoshimura, J. Sugiyama, M. Tsuta, K. Fujita, M. Shibata, M. Kokawa, S. Oshita, N. Oto, 'Prediction of Aerobic Plate Count on Beef Surface Using Fluorescence Fingerprint', *Food Bioprocess Tech.*, **7**, 1496–1504 (2014).

Encyclopedia of Analytical Chemistry, Online © 2006–2018 John Wiley & Sons, Ltd.

This article was published in the *Encyclopedia of Analytical Chemistry* in 2018 by John Wiley & Sons, Ltd.
DOI: 10.1002/9780470027318.a9540

55. A. Acharid, J. Rizkallah, L. Ait-Ameur, B. Neugnot, K. Seidel, M. Särkkä-Tirkkonen, J. Kahl, I. Birlouez-Aragon, 'Potential of Front Face Fluorescence as a Monitoring Tool of Neoformed Compounds in Industrially Processed Carrot Baby Food', *LWT Food Sci. Technol.*, **49**, 305–311 (2012).
56. C.M. Andersen, M. Vishart, V.K. Holm, 'Application of Fluorescence Spectroscopy in the Evaluation of Light-Induced Oxidation in Cheese', *J. Agric. Food Chem.*, **53**, 9985–9992 (2005).
57. J. Christensen, V.T. Povlsen, J. Sorensen, 'Application of Fluorescence Spectroscopy and Chemometrics in the Evaluation of Processed Cheese During Storage', *J. Dairy Sci.*, **86**, 1101–1107 (2003).
58. M. Loudiyi, R. Karoui, D.N. Rutledge, R. Lavigne, M.C. Montel, A. Ait-Kaddour, 'Contribution of Fluorescence Spectroscopy and Independent Components Analysis to the Evaluation of NaCl and KCl Effects on Molecular-Structure and fat Melting Temperatures of Cantal-Type Cheese', *Int. Dairy J.*, **73**, 116–127 (2017).
59. M. Tomková, J. Sádecká, K. Hroboňová, 'Synchronous Fluorescence Spectroscopy for Rapid Classification of Fruit Spirits', *Food Anal. Methods*, **8**, 1258–1267 (2015).
60. L. Lenhardt, R. Bro, I. Zekovic, T. Dramicanin, M.D. Dramicanin, 'Fluorescence Spectroscopy Coupled with PARAFAC and PLS DA for Characterization and Classification of Honey', *Food Chem.*, **175**, 284–291 (2015).
61. I. Strelec, L. Brodar, I. Flanjak, F. Čačić Kenjeric, T. Kovac, D. Čačić Kenjeric, L. Primorac, 'Characterization of Croatian Honeys by Right-Angle Fluorescence Spectroscopy and Chemometrics', *Food Anal. Methods*, **11**(3), 824–838 (2018).
62. A. Sahar, T. Boubellouta, S. Portanguen, A. Kondjoyan, É. Dufour, 'Synchronous Front-Face Fluorescence Spectroscopy Coupled with Parallel Factors (PARAFAC) Analysis to Study the Effects of Cooking Time on Meat', *J. Food Sci.*, **74**, E534–E539 (2009).
63. M.P. Ntakatsane, X.M. Liu, P. Zhou, 'Short Communication: Rapid Detection of Milk fat Adulteration with Vegetable oil by Fluorescence Spectroscopy', *J. Dairy Sci.*, **96**(4), 2130–2136 (2013).
64. A.B. Hougaard, A.J. Lawaetz, R.H. Ipsen, 'Front Face Fluorescence Spectroscopy and Multi-way Data Analysis for Characterization of Milk Pasteurized Using Instant Infusion', *LWT Food Sci. Technol.*, **53**(1), 331–337 (2013).
65. R. Yaacoub, R. Saliba, B. Nsouli, G. Khalaf, J. Rizkallah, I. Birlouez-Aragon, 'Rapid Assessment of Neoformed Compounds in Nuts and Sesame Seeds by Front-Face Fluorescence', *Food Chem.*, **115**, 304–312 (2009).
66. K.I. Poulli, G.A. Mousdis, C.A. Georgiou, 'Monitoring Olive oil Oxidation Under Thermal and UV Stress Through Synchronous Fluorescence Spectroscopy and Classical Assays', *Food Chem.*, **117**, 499–503 (2009).
67. F. Guimet, J. Ferre, R. Boque, M. Vidal, J. Garcia, 'Excitation-Emission Fluorescence Spectroscopy Combined with Three-Way Methods of Analysis as a Complementary Technique for Olive Oil Characterization', *J. Agric. Food Chem.*, **53**, 9319–9328 (2005).
68. F. Guimet, R. Boqué, J. Ferré, 'Cluster Analysis Applied to the Exploratory Analysis of Commercial Spanish Olive Oils by Means of Excitation-Emission Fluorescence Spectroscopy', *J. Agric. Food Chem.*, **52**, 6673–6679 (2004).
69. F. Ammari, C.B.Y. Cordella, N. Boughanmi, D.N. Rutledge, 'Independent Components Analysis Applied to 3D-Front-Face Fluorescence Spectra of Edible Oils to Study the Antioxidant Effect of Nigella Sativa L. Extract on the Thermal Stability of Heated Oils', *Chemom. Intell. Lab. Syst.*, **113**, 32–42 (2012).
70. N. Tena, R. Aparicio, D.L. Garcia-Gonzalez, 'Chemical Changes of Thermoxidized Virgin Olive oil Determined by Excitation-Emission Fluorescence Spectroscopy (EEFS)', *Food Res. Int.*, **45**, 103–108 (2012).
71. J.K. Eaton, A. Alcivar-Warren, J.E. Kenny, 'Multidimensional Fluorescence Fingerprinting for Classification of Shrimp by Location and Species', *Environ. Sci. Technol.*, **46**, 2276–2282 (2012).
72. S.M. Azcarate, A. de Araújo Gomes, M.R. Alcaraz, M.C. Araújo, J.M. Camiña, H.C. Goicoechea, 'Modeling Excitation–Emission Fluorescence Matrices with Pattern Recognition Algorithms for Classification of Argentine White Wines According Grape Variety', *Food Chem.*, **184**, 214–219 (2015).
73. E. Miquel Becker, J. Christensen, C.S. Frederiksen, V.K. Haugaard, 'Front-Face Fluorescence Spectroscopy and Chemometrics in Analysis of Yogurt: Rapid Analysis of Riboflavin', *J. Dairy Sci.*, **86**, 2508–2515 (2003).
74. R. Garcia, A. Boussard, L. Rakotozafy, J. Nicolas, J. Potus, D.N. Rutledge, C.B.Y. Cordella, '3D-Front-Face Fluorescence Spectroscopy and Independent Components Analysis: A new way to Monitor Bread Dough Development', *Talanta*, **147**, 307–314 (2016).
75. R. Albrecht, E. Verrecchia, H.R. Pfeiffer, 'The use of Solid-Phase Fluorescence Spectroscopy in the Characterisation of Organic Matter Transformations', *Talanta*, **134**, 453–459 (2015).
76. F. Ammari, R. Bendoula, D. Jouan-Rimbaud Bouveresse, D.N. Rutledge, J.-M. Roger, '3D Front Face Solid-Phase Fluorescence Spectroscopy Combined with Independent Components Analysis to Characterize Organic Matter in Model Soils', *Talanta*, **125**, 146–152 (2014).
77. S.K.L. Ishii, T.H. Boyer, 'Behavior of Reoccurring PARAFAC Components in Fluorescent Dissolved Organic Matter in Natural and Engineered Systems: A Critical Review', *Environ. Sci. Technol.*, **46**, 2006–2017 (2012).

Encyclopedia of Analytical Chemistry, Online © 2006–2018 John Wiley & Sons, Ltd.

This article was published in the *Encyclopedia of Analytical Chemistry* in 2018 by John Wiley & Sons, Ltd.
DOI: 10.1002/9780470027318.a9540

78. R.K. Henderson, A. Baker, K.R. Murphy, A. Hambly, R.M. Stuetz, S.J. Khan, 'Fluorescence as a Potential Monitoring Tool for Recycled Water Systems: A Review', *Water Res.*, **43**, 863–881 (2009).

79. J. Bridgeman, M. Bieroza, A. Baker, 'The Application of Fluorescence Spectroscopy to Organic Matter Characterisation in Drinking Water Treatment', *Rev. Environ. Sci. Biotechnol.*, **10**, 277–290 (2011).

80. E.M. Carstea, J. Bridgeman, A. Baker, D.M. Reynolds, 'Fluorescence Spectroscopy for Wastewater Monitoring: A Review', *Water Res.*, **95**, 205–219 (2016).

81. L. Yang, J. Hur, W. Zhuang, 'Occurrence and Behaviors of Fluorescence EEM-PARAFAC Components in Drinking Water and Wastewater Treatment Systems and Their Applications: A Review', *Environ. Sci. Pollut. Res.*, **22**, 6500–6510 (2015).

82. P.G. Coble, 'Characterization of Marine and Terrestrial DOM in Seawater Using Excitation-Emission Matrix Spectroscopy', *Mar. Chem.*, **51**, 325–346 (1996).

83. C.A. Stedmon, R. Bro, 'Characterizing Dissolved Organic Matter Fluorescence with Parallel Factor Analysis: A Tutorial', *Limnol. Oceanogr. Methods*, **6**, 572–579 (2008).

84. C.A. Stedmon, S. Markager, 'Resolving the Variability in Dissolved Organic Matter Fluorescence in a Temperate Estuary and its Catchment Using PARAFAC Analysis', *Limnol. Oceanogr.*, **50**, 686–697 (2005).

85. C.A. Stedmon, S. Markager, 'Tracing the Production and Degradation of Autochthonous Fractions of Dissolved Organic Matter by Fluorescence Analysis', *Limnol. Oceanogr.*, **50**, 1415–1426 (2005).

86. C.A. Stedmon, S. Markager, R. Bro, 'Tracing Dissolved Organic Matter in Aquatic Environments Using a new Approach to Fluorescence Spectroscopy', *Mar. Chem.*, **82**, 239–254 (2003).

87. C.A. Stedmon, S. Markager, L. Tranvik, L. Kronberg, T. Slötis, W. Martinsen, 'Photochemical Production of Ammonium and Transformation of Dissolved Organic Matter in the Baltic Sea', *Mar. Chem.*, **104**, 227–240 (2007).

88. W. Chen, P. Westerhoff, J.A. Leenheer, K. Booksh, 'Fluorescence Excitation Emission Matrix Regional Integration to Quantify Spectra for Dissolved Organic Matter', *Environ. Sci. Technol.*, **37**, 5701–5710 (2003).

89. P. Kowalczuk, M.J. Durako, H. Young, A.E. Kahn, W.J. Cooper, M. Gonsior, 'Characterization of Dissolved Organic Matter Fluorescence in the South Atlantic Bight with use of PARAFAC Model: Interannual Variability', *Mar. Chem.*, **113**, 182–196 (2009).

90. R.M. Cory, D.M. McKnight, 'Fluorescence Spectroscopy Reveals Ubiquitous Presence of Oxidized and Reduced Quinones in Dissolved Organic Matter', *Environ. Sci. Technol.*, **39**, 8142–8149 (2005).

91. S.A. Baghoth, S.K. Sharma, G.L. Amy, 'Tracking Natural Organic Matter (NOM) in a Drinking Water Treatment Plant Using Fluorescence Excitation-Emission Matrices and PARAFAC', *Water Res.*, **45**, 797–809 (2011).

92. K.R. Murphy, A. Hambly, S. Singh, R.K. Henderson, A. Baker, R. Stuetz, S.J. Khan, 'Organic Matter Fluorescence in Municipal Water Recycling Schemes: Toward a Unified PARAFAC Model', *Environ. Sci. Technol.*, **45**, 2909–2916 (2011).

93. B. Seredynska-Sobecka, C.A. Stedmon, R. Boe-Hansen, C.K. Waul, E. Arvin, 'Monitoring Organic Loading to Swimming Pools by Fluorescence Excitation Emission Matrix with Parallel Factor Analysis (PARAFAC)', *Water Res.*, **45**, 2306–2314 (2011).

94. C. Gueguen, F.A. McLaughlin, E.C. Carmack, M. Itoh, H. Narita, S. Nishino, 'The Nature of Colored Dissolved Organic Matter in the Southern Canada Basin and East Siberian Sea', *Deep-Sea Res. II Top. Stud. Oceanogr.*, **81–84**, 102–113 (2012).

95. R. Hao, H. Ren, J. Li, Z. Ma, H. Wan, X. Zheng, S. Cheng, 'Use of Three-Dimensional Excitation and Emission Matrix Fluorescence Spectroscopy for Predicting the Disinfection by-Product Formation Potential of Reclaimed Water', *Water Res.*, **46**, 5765–5776 (2012).

96. C.F. Galinha, G. Carvalho, C.A.M. Portugal, G. Guglielmi, M.A.M. Reis, J.G. Crespo, 'Two-Dimensional Fluorescence as a Fingerprinting Tool for Monitoring Wastewater Treatment Systems', *J. Chem. Technol. Biotechnol.*, **86**, 985–992 (2011).

97. M.H. Ghatee, B. Hemmateenejad, T. Sedghamiz, T. Khosousi, S. Ayatollahi, O. Seiedi, J. Sayyad Amin, 'Multivariate Curve Resolution Alternating Least-Squares As a Tool for Analyzing Crude Oil Extracted Asphaltene Samples', *Energy Fuel*, **26**, 5663–5671 (2012).

98. M. Bieroza, A. Baker, J. Bridgeman, 'Classification and Calibration of Organic Matter Fluorescence Data with Multiway Analysis Methods and Artificial Neural Networks: An Operational Tool for Improved Drinking Water Treatment', *Environmetrics*, **22**, 256–270 (2011).

99. M. Bieroza, A. Baker, J. Bridgeman, 'Exploratory Analysis of Excitation-Emission Matrix Fluorescence Spectra with Self-Organizing Maps: A Tutorial', *Educ. Chem. Eng.*, **7**, e22–e31 (2012).

100. A.J. Lawaetz, R. Bro, M. Kamstrup-Nielsen, C. Ib Jarle, N.J. Lars, J.N. Hans, 'Fluorescence Spectroscopy as a Potential Metabonomic Tool for Early Detection of Colorectal Cancer', *Metabolomics*, **8**, 111–121 (2012).

101. L. Nørgaard, G. Sölétormos, N. Harrit, M. Albrechtsen, O. Olsen, D. Nielsen, K. Kampmann, R. Bro, 'Fluorescence Spectroscopy and Chemometrics for Classification of Breast Cancer Samples—a Feasibility Study Using Extended Canonical Variates Analysis', *J. Chemometr.*, **21**, 451–458 (2007).

Encyclopedia of Analytical Chemistry, Online © 2006–2018 John Wiley & Sons, Ltd.

This article was published in the *Encyclopedia of Analytical Chemistry* in 2018 by John Wiley & Sons, Ltd.
DOI: 10.1002/9780470027318.a9540

102. P. Diagaradjane, M.A. Yaseen, J. Yu, M.S. Wong, B. Anvari, 'Autofluorescence Characterization for the Early Diagnosis of Neoplastic Changes in DMBA/TPA-Induced Mouse Skin Carcinogenesis', *Lasers Surg. Med.*, **37**, 382–395 (2005).

103. S.M. Perinchery, U. Kuzhiumparambil, S. Vemulpad, E.M. Goldys, 'The Potential of Autofluorescence Spectroscopy to Detect Human Urinary Tract Infection', *Talanta*, **82**, 912–917 (2010).

104. C. Kang, H.-L. Wu, C. Zhou, S.-X. Xiang, X.-H. Zhang, Y.-J. Yu, R.-Q. Yu, 'Quantitative Fluorescence Kinetic Analysis of NADH and FAD in Human Plasma Using Three- and Four-way Calibration Methods Capable of Providing the Second-Order Advantage', *Anal. Chim. Acta*, **910**, 36–44 (2016).

105. K. Kumazawa, H. Tabata, 'A 3D Fluorescence Analysis of the Wings of Male Morpho Sulkowskyi and Papilio Xuthus Butterflies', *Zool. Sci.*, **18**, 1073–1079 (2001).

106. M. Mularczyk-Oliwa, A. Bombalska, M. Kaliszewski, M. Wlodarski, K. Kopczynski, M. Kwasny, M. Szpakowska, E.A. Trafny, 'Comparison of Fluorescence Spectroscopy and FTIR in Differentiation of Plant Pollens', *Spectrochim. Acta A Mol. Biomol. Spectrosc.*, **97**, 246–254 (2012).

107. A. Nevin, D. Comelli, G. Valentini, R. Cubeddu, 'Total Synchronous Fluorescence Spectroscopy Combined with Multivariate Analysis: Method for the Classification of Selected Resins, Oils, and Protein-Based Media Used in Paintings', *Anal. Chem.*, **81**, 1784–1791 (2009).

108. N. Ferretto, M. Tedetti, C. Guigue, S. Mounier, R. Redon, M. Goutx, 'Identification and Quantification of Known Polycyclic Aromatic Hydrocarbons and Pesticides in Complex Mixtures Using Fluorescence Excitation-Emission Matrices and Parallel Factor Analysis', *Chemosphere*, **107**, 344–353 (2014).

109. S. Foudeil, H. Hassoun, T. Lamhasni, S.A. Lyazidi, F. Benyaich, M. Haddad, M. Choukrad, A. Boughdad, M. Bounakhla, H. Bounouira, R.M. Duarte, A. Cachada, A.C. Duarte, 'Catalog of Total Excitation–Emission and Total Synchronous Fluorescence Maps with Synchronous Fluorescence Spectra of Homologated Fluorescent Pesticides in Large use in Morocco: Development of a Spectrometric low Cost and Direct Analysis as an Alert Method in Case of Massive Contamination of Soils and Waters by Fluorescent Pesticides', *Environ. Sci. Pollut. Res.*, **22**, 6766–6777 (2015).

110. S. Elcoroaristizabal, A. de Juan, J.A. Garcia, N. Durana, L. Alonso, 'Comparison of Second-Order Multivariate Methods for Screening and Determination of PAHs by Total Fluorescence Spectroscopy', *Chemom. Intell. Lab. Syst.*, **132**, 63–74 (2014).

111. D.M. Haaland, E.V. Thomas, 'Partial Least-Squares Methods for Spectral Analyses. 1. Relation to Other Quantitative Calibration Methods and the Extraction of Qualitative Information', *Anal. Chem.*, **60**, 1193–1202 (1988).

112. F. Alarcon, M.E. Báez, M. Bravo, P. Richter, G.M. Escandar, A.C. Olivieri, E. Fuentes, 'Feasibility of the Determination of Polycyclic Aromatic Hydrocarbons in Edible Oils via Unfolded Partial Least-Squares/Residual Bilinearization and Parallel Factor Analysis of Fluorescence Excitation Emission Matrices', *Talanta*, **103**, 361–370 (2012).

113. M.L. Nahorniak, K.S. Booksh, 'Excitation-Emission Matrix Fluorescence Spectroscopy in Conjunction with Multiway Analysis for PAH Detection in Complex Matrices', *Analyst*, **131**, 1308–1315 (2006).

114. S.A. Bortolato, J.A. Arancibia, G.M. Escandar, 'Chemometrics-Assisted Excitation-Emission Fluorescence Spectroscopy on Nylon Membranes. Simultaneous Determination of Benzo[a]pyrene and Dibenz[a,h]anthracene at Parts-Per-Trillion Levels in the Presence of the Remaining EPA PAH Priority Pollutants As Interferences', *Anal. Chem.*, **80**, 8276–8286 (2008).

115. L. Rubio, M.C. Ortiz, L.A. Sarabia, 'Identification and Quantification of Carbamate Pesticides in Dried Lime Tree Flowers by Means of Excitation-Emission Molecular Fluorescence and Parallel Factor Analysis When Quenching Effect Exists', *Anal. Chim. Acta*, **820**, 9–22 (2014).

116. M.C. Rodríguez, G.H. Sánchez, M.S. Sobrero, A.V. Schenone, N.R. Marsili, 'Determination of Mycotoxins (Aflatoxins and Ochratoxin A) Using Fluorescence Emission-Excitation Matrices and Multivariate Calibration', *Microchem. J.*, **110**, 480–484 (2013).

117. J.A. Murillo Pulgarín, A. Alañón Molina, N. Boras, 'Application of non-Linear Angle Synchronous Spectrofluorimetry to the Determination of Complex Mixtures of Drugs in Urine: A Comparative Study', *Spectrochim. Acta A Mol. Biomol. Spectrosc.*, **98**, 190–198 (2012).

118. S. Warnecke, Ã. Rinnan, M. Alleso, S.B. Engelsen, 'Fluorescence Spectroscopy in Process Analytical Technology (PAT): Simultaneous Quantification of Two Active Pharmaceutical Ingredients in a Tablet Formulation', *Appl. Spectrosc.*, **69**, 323–331 (2015).

119. A. Sahar, S. Portanguen, A. Kondjoyan, E. Dufour, 'Potential of Synchronous Fluorescence Spectroscopy Coupled with Chemometrics to Determine the Heterocyclic Aromatic Amines in Grilled Meat', *Eur. Food Res. Technol.*, **231**, 803–812 (2010).

120. R. Diez, L. Sarabia, M.C. Ortiz, 'Rapid Determination of Sulfonamides in Milk Samples Using Fluorescence Spectroscopy and Class Modeling with n-way Partial Least Squares', *Anal. Chim. Acta*, **585**, 350–360 (2007).

121. D. Airado-Rodriguez, T. Galeano-Diaz, I. Duran-Meras, J.P. Wold, 'Usefulness of Fluorescence Excitation-Emission Matrices in Combination with PARAFAC, as

Encyclopedia of Analytical Chemistry, Online © 2006–2018 John Wiley & Sons, Ltd.

This article was published in the *Encyclopedia of Analytical Chemistry* in 2018 by John Wiley & Sons, Ltd.
DOI: 10.1002/9780470027318.a9540

Fingerprints of Red Wines', *J. Agric. Food Chem.*, **57**, 1711–1720 (2009).

122. R. Saad, D. Jouan-Rimbaud Bouveresse, N. Locquet, D.N. Rutledge, 'Using pH Variations to Improve the Discrimination of Wines by 3D Front Face Fluorescence Spectroscopy Associated to Independant Component Analysis', *Talanta*, **153**, 278–284 (2016).
123. R.M. Callejon, J.M. Amigo, E. Pairo, S. Garmón, J.A. Ocaña, M.L. Morales, 'Classification of Sherry Vinegars by Combining Multidimensional Fluorescence, Parafac and Different Classification Approaches', *Talanta*, **88**, 456–462 (2012).
124. U.G. Indahl, H. Martens, T. Naes, 'From Dummy Regression to Prior Probabilities in PLS-DA', *J. Chemometr.*, **21**, 529–536 (2007).
125. V. Vapnik, *The Nature of Statistical Learning Theory*, Springer-Verlag, New York, 1995.
126. Y. Gu, Y. Ni, S. Kokot, 'Solid Phase Excitation-Emission Fluorescence Method for the Classification of Complex Substances: Cortex Phellodendri and Other Traditional Chinese Medicines as Examples', *J. Phys. Chem. A*, **116**, 8949–8958 (2012).
127. G. ElMasry, H. Nagai, K. Moria, N. Nakazawa, M. Tsuta, J. Sugiyama, E. Okazaki, S. Nakauchi, 'Freshness Estimation of Intact Frozen Fish Using Fluorescence Spectroscopy and Chemometrics of Excitation–Emission Matrix', *Talanta*, **143**, 145–156 (2015).
128. G. ElMasry, N. Nakazawa, E. Okazaki, S. Nakauchi, 'Non-Invasive Sensing of Freshness Indices of Frozen Fish and Fillets Using Pretreated Excitation-Emission Matrices', *Sensors Actuators B Chem.*, **228**, 237–250 (2016).
129. E. Guzman, V. Baeten, J.A.F. Pierna, J.A. Garcia-Mesa, 'Evaluation of the Overall Quality of Olive oil Using Fluorescence Spectroscopy', *Food Chem.*, **173**, 927–934 (2015).
130. N. Tena, D.L. Garcia-Gonzalez, R. Aparicio, 'Evaluation of Virgin Olive Oil Thermal Deterioration by Fluorescence Spectroscopy', *J. Agric. Food Chem.*, **57**, 10505–10511 (2009).
131. A. Calvet, B. Li, A.G. Ryder, 'A Rapid Fluorescence Based Method for the Quantitative Analysis of Cell Culture Media Photo-Degradation', *Anal. Chim. Acta*, **807**, 111–119 (2014).
132. C.E. Comenvi, *Santé publique et Sécurité alimentaire*, European Parliament, Bruxelles, 2013.
133. C. Cordella, *Approche par empreinte et approche ciblée: deux voies complémentaires pour la sécurité sanitaire des aliments et la détection des fraudes*, Université de Nantes, Nantes, 2016.
134. J.W. White, 'Internal Standard Stable Carbon Isotope Ratio Method for Determination of C4 Plant Sugars in Honey: Collaborative Study, and Evaluation of Improved Protein Preparation Procedure', *J. AOAC Int.*, **75**, 543–548 (1992).
135. J.W. White, K. Winters, 'Honey Protein as Internal Standard for Stable Carbon Isotope Ratio: Detection of Adulteration of Honey', *J. AOAC Int.*, **72**, 907–911 (1989).
136. J.W. White, K. Winters, P. Martin, A.N. Rossmann, 'Stable Carbon Isotope Ratio Analysis of Honey: Validation of Internal Standard Procedure for Worldwide Application', *J. AOAC Int.*, **81**, 610–619 (1998).
137. Q. Chen, S. Qi, H. Li, X. Han, Q. Ouyang, J. Zhao, 'Determination of Rice Syrup Adulterant Concentration in Honey Using Three-Dimensional Fluorescence Spectra and Multivariate Calibrations', *Spectrochim. Acta A Mol. Biomol. Spectrosc.*, **131**, 177–182 (2014).
138. F. Ammari, L. Redjdal, D.N. Rutledge, 'Detection of Orange Juice Frauds Using Front-Face Fluorescence Spectroscopy and Independent Components Analysis', *Food Chem.*, **168**, 211–217 (2014).
139. D. Markechova, P. Majek, J. Sadecka, 'Fluorescence Spectroscopy and Multivariate Methods for the Determination of Brandy Adulteration with Mixed Wine Spirit', *Food Chem.*, **159**, 193–199 (2014).

Encyclopedia of Analytical Chemistry, Online © 2006–2018 John Wiley & Sons, Ltd.

This article was published in the *Encyclopedia of Analytical Chemistry* in 2018 by John Wiley & Sons, Ltd.
DOI: 10.1002/9780470027318.a9540